Investigations of Environmental Effects on Freeway Acoustics

Final Report 605(1)

Prepared by:

H.J.S. Fernando
Center for Environmental Fluid Dynamics,
Arizona State University,
Tempe, AZ 85287-9809

N.C. Ovenden
Department of Mathematics,
University College London,
Gower Street, London WC1E 6BT, U.K.

S.R. Shaffer
Center for Environmental Fluid Dynamics,
Arizona State University,
Tempe, AZ85287-9809

March 2010

Prepared for:
Arizona Department of Transportation
in cooperation with
U.S. Department of Transportation
Federal Highway Administration

Research Center reports are available on the Arizona Department of Transportation's internet site.

Technical Report Documentation Page

1. Report No.	2. Government Accession No.	3. Recipient's Catalog No.
FHWA-AZ-10-605(1)		

4. Title and Subtitle	5. Report Date
Investigations of Environmental Effects on Freeway Acoustics	March 2010
	6. Performing Organization Code

7. Author	8. Performing Organization Report No.
H.J.S. Fernando, N. Ovenden, S. Shaffer	

9. Performing Organization Name and Address	10. Work Unit No.
Arizona State University Office for Research & Sponsored Projects Administration P.O. Box 873503 Tempe, AZ 85287-3503	11. Contract or Grant No. SPR-PL-1(69)ITEM 605

12. Sponsoring Agency Name and Address	13.Type of Report & Period Covered
Arizona Department of Transportation 206 S. 17th Avenue Phoenix, Arizona 85007	Final Report 05/04/2006 to 06/02/2008
	14. Sponsoring Agency Code

15. Supplementary Notes

Prepared in cooperation with the U.S. Department of Transportation, Federal Highway Administration

16. Abstract

The study reported here was designed to examine the impact of background meteorological conditions on the propagation of noise from urban freeways in the Phoenix area. The aim was to understand and predict how sound waves emanating from highways respond to the vertical profiles of atmospheric temperature gradients and velocity shear, so that sound measurements can be interpreted with regard to the environmental variability. Over the course of four days in late 2006 and two days in early 2007, field experiments were carried out at two freeway sites, where meteorological data and sound levels were measured and recorded from early morning until the middle of the day. Such periods span the stable, morning transitional and convective periods of the atmosphere. From the data collected, three test cases of varying atmospheric density stratification and wind shear are presented and discussed. These cases represent all measurement periods and were analyzed in detail.

A parabolic equation model coupled to a Green's function model close to the source field was developed and used to compute the refracted sound field for experimental cases up to half a mile from the freeway, permitting computations of noise exposure of residential areas nearby. The model demonstrates that atmospheric effects are able to raise sound levels by 10dB–20dB at significant distances from the highway, which at times led to exceeding acceptable limits imposed by Federal Highway Administration for residential areas. Mitigation strategies such as barriers and asphalt rubber friction course (ARFC) are also briefly discussed.

17. Key Words	18. Distribution Statement	23. Registrant's Seal
Noise propagation, meteorological effects, acoustic modeling, field studies, noise exposure, mitigation strategies, freeway noise	Document is available to the U.S. public through the National Technical Information Service, Springfield, Virginia, 22161	

19. Security Classification	20. Security Classification	21. No. of Pages	22. Price
Unclassified	Unclassified	50	

SI (MODERN METRIC) CONVERSION FACTORS*

APPROXIMATE CONVERSIONS TO SI UNITS

Symbol	When You Know	Multiply By	To Find	Symbol
	LENGTH			
in	inches	25.4	millimeters	mm
ft	feet	0.305	meters	m
yd	yards	0.914	meters	m
mi	miles	1.61	kilometers	km
	AREA			
in^2	square inches	645.2	square millimeters	mm^2
ft^2	square feet	0.093	square meters	m^2
yd^2	square yards	0.836	square meters	m^2
ac	acres	0.405	hectares	ha
mi^2	square miles	2.59	square kilometers	km^2
	VOLUME			
fl oz	fluid ounces	29.57	milliliters	mL
gal	gallons	3.785	liters	L
ft^3	cubic feet	0.028	cubic meters	m^3
yd^3	cubic yards	0.765	cubic meters	m^3
	NOTE: Volumes greater than 1000L shall be shown in m^3.			
	MASS			
oz	ounces	28.35	grams	g
lb	pounds	0.454	kilograms	kg
T	short tons (2000lb)	0.907	megagrams (or "metric ton")	mg (or "t")
	TEMPERATURE (exact)			
°F	Fahrenheit temperature	5(F-32)/9 or (F-32)/1.8	Celsius temperature	°C
	ILLUMINATION			
fc	foot candles	10.76	lux	lx
fl	foot-Lamberts	3.426	candela/m^2	cd/m^2
	FORCE AND PRESSURE OR STRESS			
lbf	poundforce	4.45	newtons	N
lbf/in^2	poundforce per square inch	6.89	kilopascals	kPa

APPROXIMATE CONVERSIONS FROM SI UNITS

Symbol	When You Know	Multiply By	To Find	Symbol
	LENGTH			
mm	millimeters	0.039	inches	in
m	meters	3.28	feet	ft
m	meters	1.09	yards	yd
km	kilometers	0.621	miles	mi
	AREA			
mm^2	Square millimeters	0.0016	square inches	in^2
m^2	Square meters	10.764	square feet	ft^2
m^2	Square meters	1.195	square yards	yd^2
ha	hectares	2.47	acres	ac
km^2	Square kilometers	0.386	square miles	mi^2
	VOLUME			
mL	milliliters	0.034	fluid ounces	fl oz
L	liters	0.264	gallons	gal
m^3	Cubic meters	35.315	cubic feet	ft^3
m^3	Cubic meters	1.308	cubic yards	yd^3
	MASS			
g	grams	0.035	ounces	oz
kg	kilograms	2.205	pounds	lb
mg	megagrams (or "metric ton")	1.102	short tons (2000lb)	T
	TEMPERATURE (exact)			
°C	Celsius temperature	1.8C + 32	Fahrenheit temperature	°F
	ILLUMINATION			
lx	lux	0.0929	foot-candles	fc
cd/m^2	candela/m^2	0.2919	foot-Lamberts	fl
	FORCE AND PRESSURE OR STRESS			
N	newtons	0.225	poundforce	lbf
kPa	kilopascals	0.145	poundforce per square inch	lbf/in^2

SI is the symbol for the International System of Units. Appropriate rounding should be made to comply with Section 4 of ASTM E380

TABLE OF CONTENTS

LIST OF FIGURES

ACKNOWLEDGMENTS

We are extremely grateful to Arizona Department of Transportation (ADOT), Arizona State University (ASU), and University College London (UCL) for their support of this ongoing collaborative research. In particular, we thank Christ Dimitroplos, Fred Garcia, and Lisa Anderson at ADOT for their interest and encouragement. The consultant Illingworth & Rodkin's assistance in the project in measuring and processing the sound data is also gratefully acknowledged and we also thank Dragan Zajic, Leonard Montenegro, and Adam Christman for their help with the field experiments and subsequent data analysis.

EXECUTIVE SUMMARY

The study reported here was designed to examine the impact of background meteorological conditions on the propagation of noise from urban freeways in the Phoenix area. The aim was to understand and predict how sound waves emanating from highways respond to the vertical profiles of atmospheric temperature gradients and velocity shear, so that sound measurements can be interpreted with regard to the environmental variability. Over the course of four days in late 2006 and two days in early 2007, field experiments were carried out at two freeway sites, where meteorological data and sound levels were measured and recorded from early morning until the middle of the day. Such periods span the stable, morning transitional and convective periods of the atmosphere. From the data collected, three test cases of varying atmospheric density stratification and wind shear are presented and discussed. These cases represent all measurement periods and were analyzed in detail.

A parabolic equation model coupled to a Green's function model close to the source field was developed and used to compute the refracted sound field for experimental cases up to half a mile from the freeway, permitting computations of noise exposure of residential areas nearby. The model demonstrates that atmospheric effects are able to raise sound levels by 10dB–20dB at significant distances from the highway, which at times led to exceeding acceptable limits imposed by the Federal Highway Administration (FHWA) for residential areas. Mitigation strategies such as barriers and asphalt rubber friction courses (ARFC) are also briefly discussed.

I. INTRODUCTION

Noise pollution is a serious and worsening environmental concern in urban areas. Not only does it diminish the quality of human life,[1,2,3] but it also alters wildlife habitats.[4] Highway traffic, airports, heavy industry, railways, and even leisure activities located close to built-up areas all contribute to the noise menace, and thus urban planners and managers pay close attention to mitigate it. This report concerns a study on a significant contributor to noise pollution in urban areas — freeway traffic noise — which varies considerably.

The noise level depends upon a myriad of factors, such as ground conditions; terrain and the presence of sound barriers; temporal variations in traffic speed, volume, and vehicle types; and also spatiotemporal variation of meteorological variables such as temperature, wind velocity, and turbulence.[5,6] While some of these factors are accounted for in operational sound prediction models, available operational models do not take all salient factors into account.[7,8] For example, the latest version of the Federal Highway Administration's (FHWA) Traffic Noise Model (TNM)[9] (Version 2.5 released in 2004) does not account for the effects of temperature and wind variability: uniform, isothermal atmospheric conditions are assumed in the calculations. The latter is a reasonable assumption for shorter (less than 650 ft (198 m) distances from the sound source, but errors can be substantial when predicting intermediate and far field noise. This drawback is of particular importance when refraction of sound due to temperature and wind causes anomalous intensity variations of sound at distance from the source. For example, noise measurements and analysis conducted in Scottsdale, Arizona, following complaints by residents living more than ¼ mile (about 400 m) from the eastern portion of Loop 101, suggest that ground-level inversions (surface stable temperature stratification) can increase the sound level by as much as 10 decibels to 15 decibels (dB).[10]

While the noise level under neutral atmospheric conditions is well within the Federal Highway Administration (FHWA) noise abatement criterion (NAC), an inversion can cause decibel levels to violate the standard. FHWA-NAC recommends implementing abatement procedures such as noise walls or modified pavement types (quiet pavements) when the energy averaged or equivalent sound level (L_{eq}) approaches a value of 67 A-weighted decibels (dBA). (A-weighting is used to account for typical human sensitivity to various frequencies of absolute pressure fluctuations following ISO standard IEC 651 (1993-09) by applying a band-pass filter. Note that when referring to a difference in sound pressure levels, dB are interchangeable with dBA.) Such levels can be observed at some distance around certain Arizona freeways merely as a result of inversions and wind shear.

The influence of atmospheric factors becomes particularly critical when noise mitigation is realized via a combination of techniques, for example, noise walls and quiet pavements. The Arizona Department of Transportation (ADOT) has received approval from the FHWA for the Quiet Pavement Pilot Program (QPPP) to investigate the usefulness of pavement-surface type as a noise mitigation strategy, subject to the condition that Arizona would be a pilot program with specific research objectives and requirements.[40] This research is intended to validate the efficacy of asphalt rubber friction courses (ARFC) as a noise mitigation method. Over several years ADOT will overlay Portland cement concrete

pavement (PCCP) in metropolitan Phoenix with a 1-inch–thick ARFC surface. Where the ARFC is placed and noise walls are required, the walls may be reduced in height in view of the extra mitigation offered by ARFC surfacing.[40]

Sound barrier walls, also known as sound walls, are designed to protect the public and particularly the nearby residents against noise pollution, which is adverse sound level exposure that can lead to hearing loss, sleep disturbance, stress, and increased blood pressure. To decrease noise pollution effects, regulations have been instituted by governments. Such statutes in the United States include the U.S. National Environmental Policy Act, the Federal-Aid Highway Act, and the Noise Control Act of 1972. These acts have promoted decreased noise pollution, quantitative noise analyses, use of sound barrier walls, and city noise planning. A well-designed noise wall diffracts and reflects sound waves to optimize the attenuation of far field sound. To determine if sound barrier walls are effective, the sound is allowed to pass through or over the wall and the transmitted noise levels are gauged. When a 9dB reduction is reached, a sound barrier wall is considered adequate. Nine decibels lower in sound is equal to approximately a 90 percent drop in sound waves traveling past the wall.

Beginning in 2003, ADOT has been monitoring six sites across the Phoenix metropolitan area for traffic-generated noise over a 10-year period to evaluate the effectiveness of ARFC. While measurements show that ARFC has reduced freeway noise appreciably (8dB–10dB) at close-in and community locations, sound refraction due to environmental conditions can defeat the noise abatement approaches (e.g., the use of walls) at some distances away. In such instances, noise walls would be of little help as a mitigation tool and, as noise walls are expensive, the merits of their installation should be carefully evaluated *a priori*.

ARFC pavements, sound walls, and environmental factors become dominant only at certain intrinsic frequency ranges. The relationships between these variables and A-weighted noise levels in the field thus are intricate and can be delineated only via models that properly quantify fundamental relationships and their complex interactions. It is therefore important to develop scientific knowledge and tools to predict atmospheric effects on freeway noise that help evaluate alternative design options. Such tools will also help with interpretation of measurements taken at different positions and/or times and in placing results on a unified scientific basis (i.e., in terms of a certain base or standard state). The only viable method for predicting sound in complex field situations is the use of a numerical model that incorporates all governing factors, the straightforward (yet onerous) method in this context being nesting of an acoustic model with an environmental forecasting model. Such a modeling system is prohibitively computer intensive and so can be invoked only under very special circumstances. A simpler method is to use available representative atmospheric data from the area to feed the acoustic model, assuming local smaller scale variations are unimportant. The research reported here is of this type and includes a meteorological measurement component. This study's aim was to examine how different meteorological conditions, especially ground-based inversions, can affect freeway noise under high-pressure, low-synoptic flow conditions prevalent in the desert Southwest.[11,12] The study was particularly motivated by the Quiet Pavement Pilot

Program, where the noise reduction capabilities of the rubber friction course are being measured over a decade. To put results into a consistent framework, the meteorological effects need to be included in presenting the noise results.

Although physical mechanisms underlying atmospheric sound propagation are well understood, the lack of both sufficiently detailed atmospheric data and computer models capable of incorporating them into an integrated formulation have hampered progress on modeling the impact of environmental effects on sound propagation. A review of literature suggests that:

- for downwind propagation, the magnitude of sound fluctuations increases with the frequency of the signal and with distance;
- for upwind propagation, the fluctuations are greatest near the shadow boundary;
- in a stable atmosphere (clear night, weak winds) the range of fluctuations is typically about 5dB, mainly due to the gravity waves and turbulence, but sound levels can be enhanced due to refraction at distances beyond ¼ mile (400 m);
- in an unstable atmosphere (clear sunny day, strong winds) the range of fluctuation is typically 15dB–20dB;
- the spectrum of fluctuations measured over open ground encompasses a range of frequencies that humans can hear from 50 Hz to above 3 kHz; and
- sound propagation from hilltop to hilltop and from air to ground is frequently characterized by large low-frequency fluctuations.

A suite of computational approaches is being used for atmospheric sound propagation studies,[5] which include:

Gaussian beam methods — this is a variant of the classical ray tracing technique by solving the wave equation in the neighborhood of the conventional rays and associating a Gaussian amplitude profile normal to each ray. An approximate overall solution can then be constructed as a superposition of these so-called beams.

Fast Field Program Models (FFP) — a semi-analytical method involving computation of the sound field in a horizontally layered homogeneous atmosphere in horizontal wave number domain, which is then inverted to the spatial domain using an inverse Fourier transform.

Parabolic Equation (PE) models — a marching solution based on splitting the governing wave equations into left- and right-traveling components, originating at the source and capable of being "perturbed" en route to account for topography, barriers, and turbulence.

Ray theories, although robust for indoor acoustics, rapidly become highly cumbersome to compute in downward refracting media where many rays are needed and caustics are problematic. Additional complications, such as diffraction by obstacles, turbulence, and prediction of acoustic shadow regions, further urge the use of alternative methods. The key to PE models is the use of an effective sound speed based upon temperature and wind speed of the actual mean flow field, both of which modify the isotropic adiabatic sound speed.[13,14]

When assuming a line (or axisymmetric) source, the two-dimensional wave operator is factored into left- and right-traveling components transverse to the source. The pressure field due to a source can then be resolved in the domain by marching the solution numerically away from the source, while discounting any waves that propagate towards the source. Major disadvantages of this method are that it becomes inaccurate at high elevation angles and cannot directly account for back scatter unless the more difficult task of handling propagation in both directions is addressed. It has many advantages, however, including the ease of incorporating atmospheric absorption and varying boundary conditions and geometries, along with actual spatially varying meteorological profiles. Extensions that incorporate turbulence and flow details, such as over a barrier or rough terrain (e.g., large eddy simulations) have also begun to be incorporated into the scheme. For these reasons, methodologies based on the PE equation prove highly popular.[15-21]

The FFPs typically have a faster run time than their PE counterparts and can handle realistically complicated vertical atmospheric profiles. They can also account for the vectorial nature of the mean flow without requiring an "effective" sound speed and are accurate at high elevation angles. However, the required Fourier transformation in the horizontal direction means that the model is restricted to homogeneous ground surfaces, with a flat topography containing at most a single and relatively simple topographical feature.[22-27] It is common to use hybrids—models that combine several methods—to address aspects of the problem at hand in an attempt to circumvent potential drawbacks of any individual method.[5, 28-32]

In order to understand and quantify the effects of atmospheric temperature and velocity profiles on sound propagation, refraction, and diffraction, we have combined a field measurement campaign with modeling efforts. The field measurements are to provide realistic vertical profiles of temperature and cross wind velocities to the model and were performed over six days at two freeway sites in Scottsdale, Arizona, and Mesa, Arizona, where meteorological and sound data were taken and recorded over roughly a six-hour period between 6am and 12pm. For the modeling, the sound data is entered into a Green's function model to evaluate the near source field generated from the freeway traffic. This source field, along with the meteorological data, is then input into a parabolic equation (PE) model to compute the refracted sound field out to a distance of 1968 ft (600 m). The results are compared to neutral atmospheric conditions; the effect of stratification and wind shear are separated and quantified in three 20-minute time-averaged cases selected from the field data.

The outline of this report is as follows. The field experiments and equipment used are described in detail in Section II. Section III briefly outlines the acoustic propagation model. The selection of the three test cases to be entered into the model is presented in Section IV. The procedure of using sound measurements to construct a near-source field using a Green's function model and calculated ground impedance is given in Section V. The evolution of the noise frequency spectra with range and the construction of overall L_{eq} plots are then presented in Section VI. Finally, conclusions, recommendations to ADOT, and plans for future work are described in Section VII.

II. EXPERIMENTS

To study the influence of meteorological conditions on noise propagation from Phoenix highways, the Center for Environmental Fluid Dynamics at Arizona State University (EFD-ASU) conducted a joint field campaign with ADOT and Illingworth & Rodkin, Inc. The EFD-ASU team provided detailed measurements of atmospheric meteorological conditions, while Illingworth & Rodkin, Inc. provided sound measurements. ADOT staff videotaped the traffic and recorded its speed. Field measurements were taken at two different sites along highways in the Phoenix metropolitan area. The sites are standard designated sites for ADOT, and the details of these sites are outlined in Saurenman et al.[10]

The first series of measurements was taken on October 10 and 11, 2006, on the west side of Loop 101 at milepost 47 (ADOT location site 3E). The second series was carried out on November 7 and 8, 2006, on the north side of Loop 202 (ADOT location 3D). The third series was on March 20 and 21, 2007, again at the Phoenix Loop 202 site. Figure 1 shows the location of the sites on the metropolitan Phoenix freeway system. Figure 2 shows maps of both locations with red dots indicating the approximate measurement sites. Both sites have a relatively flat homogeneous terrain (see cross-sectional profiles in Figures 3 and 4) with hard sandy soil and sparse bushes. However, away from the sites is complex topography that may alter the meteorological variables. Measurements were taken from 7am to 11am, and beginning at 6am for the two days in March, in order to better understand how noise levels change with atmospheric conditions. The earliest time for the start of the experiment was determined by the logistical constraints of the contractor. The goal was to obtain data during periods of temperature inversion, typical daytime adiabatic lapse conditions, and morning transition, covering representative periods of the months concerned. It is interesting to note that the temperature conditions near the surface were found to be unstable even in the early morning hours, and this is believed to be due to turbulent mixing and heat retention of the freeway surface. Further work is necessary to investigate such features.

A number of instruments were employed, which included three-dimensional sonic anemometers, a meteorological balloon with tethersonde system, and a SODAR (SOund Detection And Ranging) with RASS (Radio Acoustic Sounding System) attachment. Sound measurement instruments were located at distances of 50 ft and 100 ft from the center of the nearest lane of the highway at the 3E site and 50 ft, 100 ft, and 250 ft (15.24 m, 30.48 m, and 76.2 m) from the center of the nearest lane at the 3D site. The sonic anemometers were located on towers at the same distance from the highway as the sound measurement instruments. Tethersonde and SODAR/RASS systems were located slightly further away to avoid contamination of sound-level measurements. Schematics of the cross-sectional area of the sites are given in Figures 3 and 4. Figure 5 has photographs of the instruments employed.

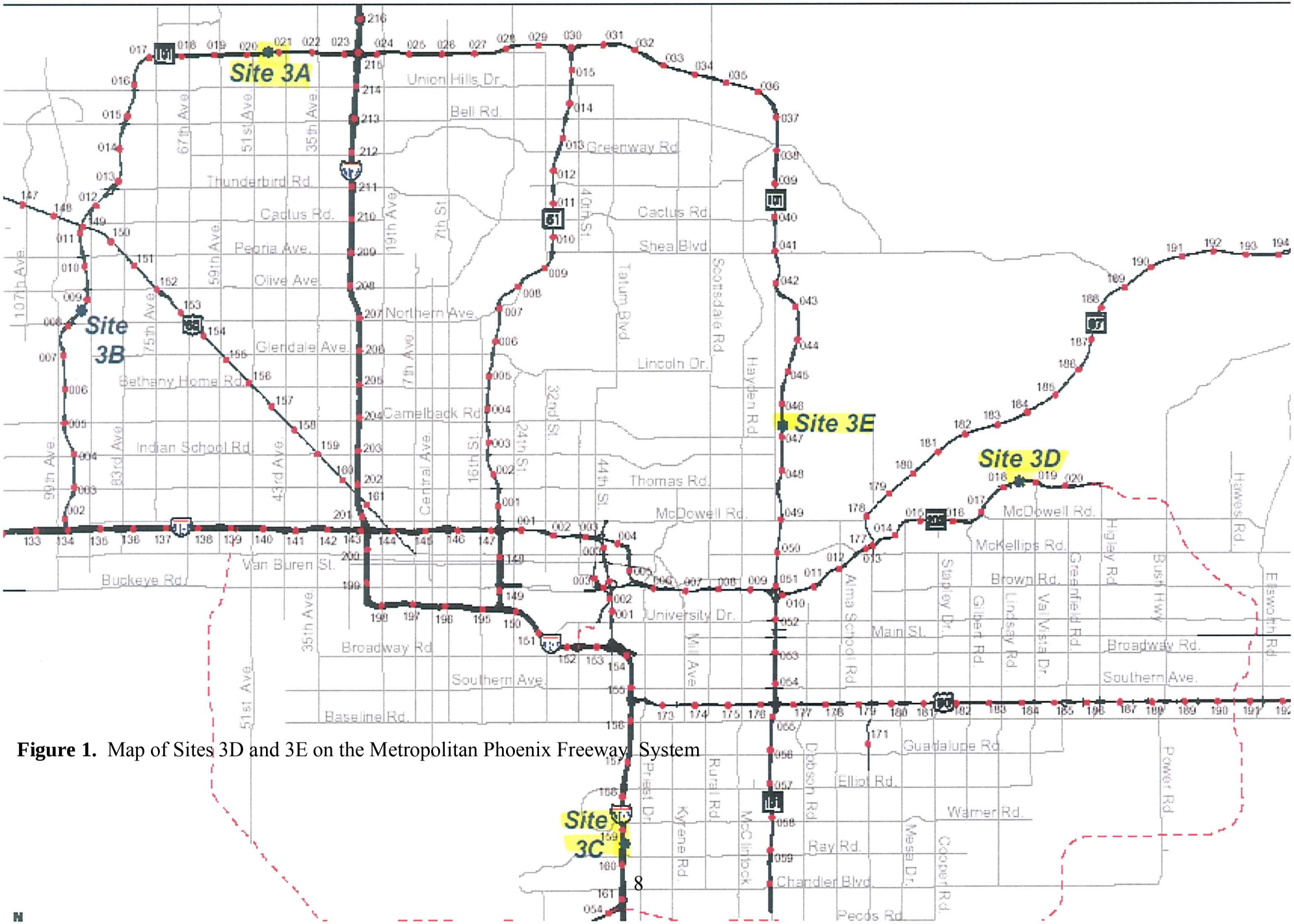

Figure 1. Map of Sites 3D and 3E on the Metropolitan Phoenix Freeway System

Figure 2. Location maps for Loop 101 (top; location site 3E) and Loop 202 (bottom; location site 3D). The red dot indicates the approximate location of the measurement sites.

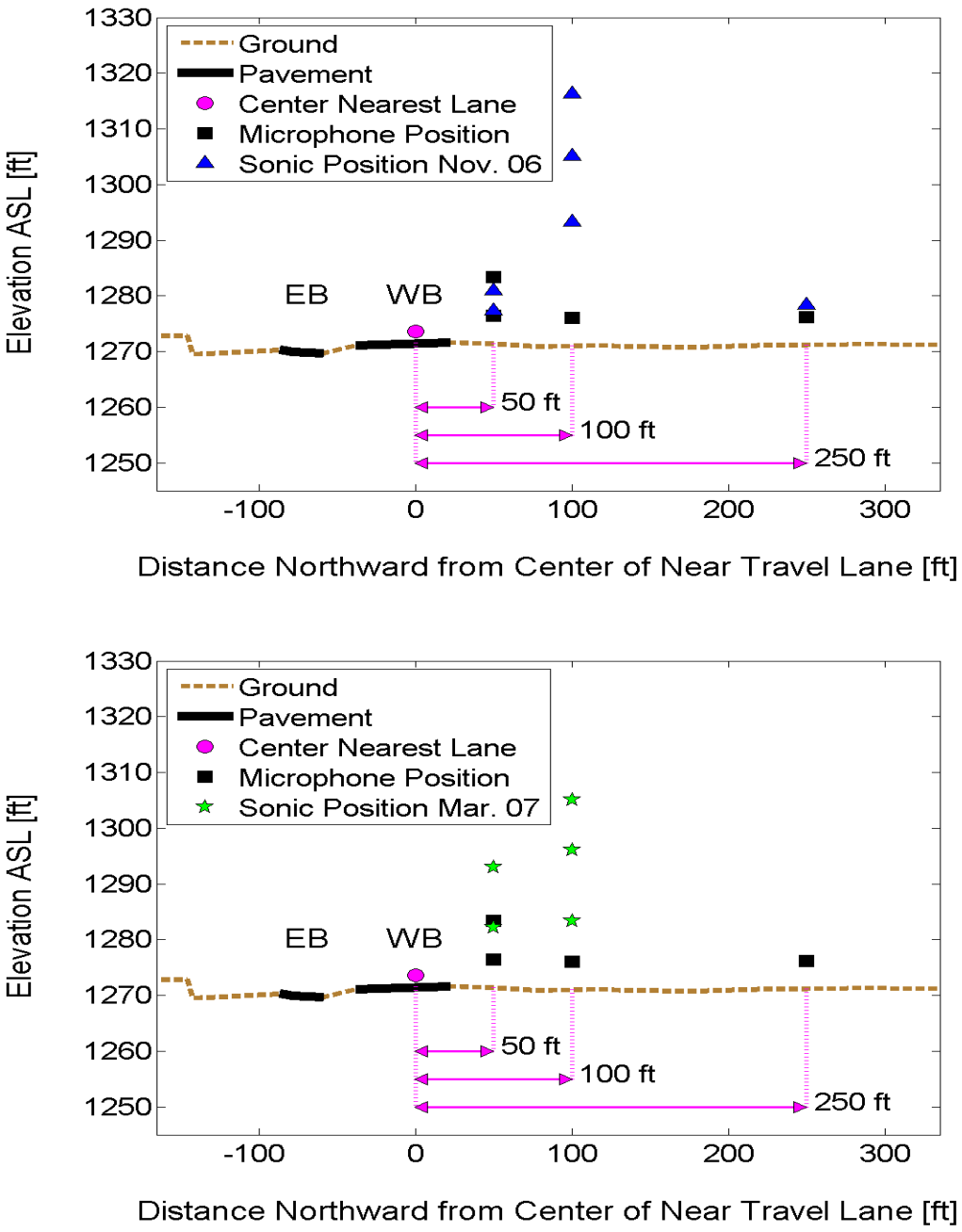

Figure 3. Cross section for Loop 202 location expressed as the elevation above sea level (ASL) (in feet). Horizontal distance is shown measured in feet from the fence on the north side. Positions of instruments are shown as squares for microphones, triangles and stars for sonic anemometers in November (top) and March (bottom), respectively. Arrows indicate horizontal distances of 50 ft, 100 ft, and 250 ft from the center of the nearest travel lane on the westbound (WB) side.

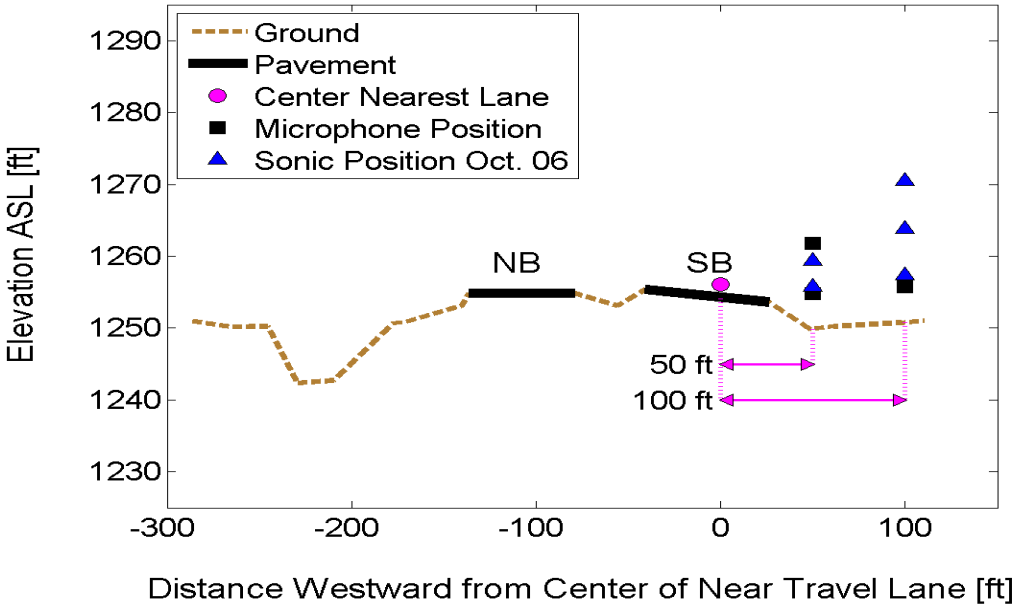

Figure 4. Location cross section for Loop 101 expressed as the elevation above sea level. Horizontal distance is shown measured in feet from the fence on the west side. Positions of instruments are shown as squares for microphones and triangles for sonic anemometers in the October 2006 field campaign. Arrows indicate horizontal distances of 50 ft and 100 ft from the center of the nearest travel lane on the southbound (SB) side.

Figure 5. Photographs of instruments deployed in the experiment. Two sonic anemometers on a short tripod on right side, and two microphones on the tripod in the left side of the picture, at Loop 202 in November 2006 (top); and the SODAR-RASS system at Loop 101 in October (bottom).

Figure 6. Photograph of the balloon-tethersonde system used at the Loop 101 site in October 2006.

The balloon and tethersonde system is an important tool in atmospheric boundary-layer studies since it provides detailed profiles of wind speed, wind direction, temperature, air pressure, and humidity in the lower atmosphere. During the two days of field experiments in October, the balloon system shown in Figure 6 was deployed with a single tethersonde, thus providing profiles of temperature, wind speed and direction, and atmospheric pressure, and the data could be obtained up to 164 ft (50 m) above ground level (agl). The allowable height of balloon flights was determined by the FAA air traffic permit. However, due to problems with a malfunctioning sonde on the second day, the balloon-tethersonde system was used only during these two days of measurements. Also, during the first day, there was a period of stronger winds when the balloon was not used due to safety reasons. Comparison of sonic anemometer data located on the tower with those obtained by the balloon system show a good agreement, and hence the data from the sonic anemometers were used for velocity calculations when the balloon system was inoperative.

The sonic anemometers were operated at a frequency 10 Hz, providing all three velocity components (one in each dimension U_x, U_y, U_z) and temperature. The large frequency of measurements provided an opportunity to obtain information on mean flow and temperature close to the surface, as well as properties of the turbulence. The latter was used to calculate turbulence statistics, such as the root mean square for velocities and temperature, as well as for turbulent momentum and heat fluxes. The sonic anemometer placement is discussed below.

(i) October 10 and 11 — two sonic anemometers were located on a tripod 50 ft (15.24 m) and three on a meteorological tower 100 ft (30.48 m) from the center line of the closest travel lane. The heights of instruments on the tripod were 5.9 ft and 9.5 ft (1.8 m and 2.9 m) agl and the heights of those on the tower were 6.6 ft, 13.2 ft and 19.7 ft (2 m, 4 m and 6 m) agl.

(ii) November 7 and 8 — an additional tripod was also located closest to the highway 50 ft (15.24 m) where the heights of sonic anemometers were 5.9 ft and 9.5 ft (1.8 m and 2.9 m) agl, while sonic anemometers at the tower were placed at levels 22.3 ft, 34.1 ft and 45.3 ft (6.8 m, 10.4 m and 13.8 m) agl. On November 8, one more sonic was placed on a tripod at a location 250 ft (76.20 m) from the center of the near lane at 7.2 ft (2.2 m) agl in order to measure atmospheric conditions close to the farthest sound measurement point.

(iii) March 20 and 21 — two towers were set up at distances of 50 ft and 100 ft (15.24 m and 30.48 m) from the center of the near lane. Two sonic anemometers were positioned at heights of 10.8 ft and 21.6 ft (3.30 m and 6.60 m) agl on the tower closest to the roadway, while three sonic anemometers at 12.4 ft, 25.1 ft and 34.1 ft (3.78 m, 7.65 m and 10.39 m) agl were used on the farthest tower. In some cases, the sonic anemometers did not work properly, and data from these periods were not included in the data set and subsequent analysis.

The SODAR/RASS system was utilized to measure wind speed and temperature profiles between roughly 65 ft to 1968 ft (20 m to 600 m) agl. This system was used in order to provide more details on the structure of the atmospheric boundary layer at greater heights, but for the present study the most important were data near the lowest 328 ft (100 m) or so.

III. MODELING

Based on sound data from field experiments provided by Illingworth & Rodkin, a two-dimensional model can be constructed on acoustic propagation from a single mono-frequency coherent line source in a vertically layered atmosphere. A rectangular *xy* coordinate system is used, with *y* measuring the vertical height and *x* measuring the horizontal range from the center line of the near lane of the highway. All lengths are non-dimensionalized on a typical source height L_0, velocities are non-dimensionalized on the sound speed measured at the ground level C_0, density is non-dimensionalized on the density of air at 1 atmosphere (ρ_0=1.2 kg m^{-3}) and pressure p is non-dimensionalized on $\rho_0 C_0^2$. For a given frequency f Hz, we define the Helmholtz number as $\omega = 2\pi f L_0/C_0$ and by writing the acoustic pressure perturbation as $p(x,y,t)=p_c(x,y)e^{-i\omega t}$, the Helmholtz equation for a line source at $\boldsymbol{x}=\boldsymbol{x_0}$ of strength S in a vertically layered atmosphere is obtained as

$$\frac{\partial^2 p_c}{\partial x^2} + \frac{\omega^2}{\tilde{c}^2(y)} \frac{\partial}{\partial y}\left(\frac{\tilde{c}^2(y)}{\omega^2} \frac{\partial p_c}{\partial y} \right) + \frac{\omega^2}{\tilde{c}^2(y)} p_c = S\delta(x - x_0). \qquad (1)$$

Here, $\tilde{c}$ is the non-dimensional *effective* sound speed, which includes the effects of both temperature and crosswind. Given a measured vertical temperature profile $T(y)$ and crosswind speed profile $U_0(y)$, the effective sound speed is defined in a standard manner to be

$$\tilde{c}(y) = \frac{\sqrt{\gamma R T(y)} + U_0(y)}{c_0}$$

where γ is the ratio of specific heats and R is the ideal gas constant. The boundary conditions imposed are a far-field Sommerfeld radiation condition as $r = \sqrt{x^2 + y^2}$ becomes large, of the form

$$\frac{\partial p_c}{\partial r} - i\frac{\omega}{\tilde{c}} p_c = o\left(r^{-1/2}\right) \text{and } p_c = 0\left(r^{-1/2}\right) \text{as } r \to \infty \qquad (2)$$

and an impedance boundary condition at the surface

$$-\frac{1}{i\omega}\frac{\partial p_c}{\partial y} = \frac{1}{Z} p_c \text{ at } y = 0$$

Throughout this report, the empirical impedance model of Delany and Bazley[33] is used where, for a ground surface with flow resistivity σ [Pa s m^{-2}], the impedance Z is given by

$$Z = 1 + 0.0511\left(\frac{\sigma}{f}\right)^{0.75} + i0.0768\left(\frac{\sigma}{f}\right)^{0.73} \qquad (4)$$

Two models are used in tandem to compute the far-field sound propagation: (i) a near-field Green's function method assuming a homogeneous atmosphere and (ii) a parabolic equation approximation. Figure 7 shows the regions of the *xy* domain where each model is used.

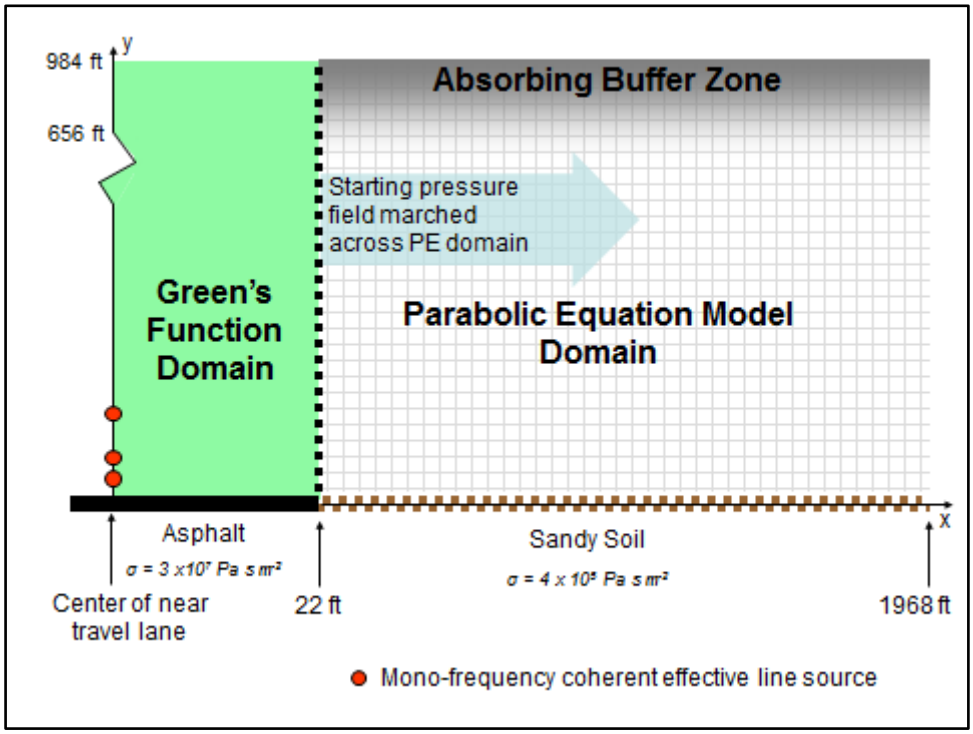

Figure 7. A schematic of the coupled models used to resolve the far-field propagation of traffic noise from a freeway corridor. The red dots represent monofrequency coherent effective line sources positioned above the center of the nearest lane of traffic.

The near-field Green's function method[34] is used to obtain the acoustic field in the vicinity of the line source where the refractive effects of atmospheric factors can be assumed to be negligible. In other words, the Green's function method assumes a constant effective sound speed $c=1$ and solves equations (1) to (3) with this assumption up to the edge of the highway, at 22 ft (6.7 m), obtaining the sound field

$$p_c(x,y;y_0) = -\frac{1}{4}H_0^{(1)}\left(\omega\sqrt{x^2+(y-y_0)^2}\right) - \frac{i}{4}H_0^{(1)}\left(\omega\sqrt{x^2+(y+y_0)^2}\right) + P_Z(x,y;y_0) \quad (5)$$

where $H_0^{(1)}$ is the zeroth order Hankel function of the first kind, and the term $P_Z(x,y;y_0)$ represents the correction to the hard-wall solution for finite *z*. This correction is derived by Chandler-Wilde and Hothersall[34] and is given in terms of

$$\lambda = \omega\sqrt{x^2 + (y + y_0)^2},$$
$$\gamma = (y + y_0)/\omega\sqrt{x^2 + (y + y_0)^2}$$
$$a_+ = 1 + \frac{\gamma}{Z} - \left(1 - Z^{-2}\right)^{1/2}\left(1 - \gamma^2\right)^{1/2}$$

with the result

$$P_Z(x, y; y_0) = \frac{e^{i\lambda}}{\pi Z\sqrt{\lambda}}\int_0^\infty s^{-1/2}e^{-s}g(s/\lambda)ds + \frac{e^{i\lambda(1-a_+)}}{2\sqrt{Z^2 - 1}}erfc\left|e^{-i\pi/4}\sqrt{\lambda a_+}\right|$$

where

$$g(t) = -\frac{\left[Z^{-1} + \gamma(1 + it)\right]}{(t - 2i)^{1/2}\left[t^2 - 2i(1 + \gamma/Z)t - (Z^{-1} + \gamma)^2\right]} - \frac{e^{-i\pi/4}\sqrt{a_+}}{2(1 - Z^{-2})^{1/2}(t - ia_+)}$$

The first integral expression is calculated using Gauss-Laguerre Quadrature and the second *surface wave* term (due to its strong exponential decay away from the ground) is evaluated using the formula given in Attenborough.[35] Assume over the near-field calculation, the ground impedance is typically of porous asphalt with $\sigma = 3\text{x}10^7$ Pa s m^{-2}, which is given in Table 4.9 of Attenborough.[6]

The near-field Green's function model provides an acoustic field at the edge of the freeway $p_{ini}(y)=p_c(x_{edge},y)$, which is subsequently used as an initial condition for a two-dimensional Cartesian variant of the standard axisymmetric parabolic equation (PE) model, first derived by Gilbert and White.[13]

The PE model used is the parabolic wide-angle approximation of (1) assuming a two-dimensional line source. The pressure field is rewritten as $p_c(x,y)=\psi(x,y)\, e^{i\omega x}$ and $\psi(x,y)$ is obtained by solving the equation

$$\frac{\partial\psi}{\partial x} + \frac{1}{4\omega^2}\left[\frac{1}{\tilde{c}^2}\frac{\partial}{\partial y}\left(\tilde{c}^2\frac{\partial^2\psi}{\partial y\partial x}\right) + \omega^2\left(\frac{1}{\tilde{c}^2} - 1\right)\frac{\partial\psi}{\partial x}\right] = \frac{i}{2\omega}\left[\frac{1}{\tilde{c}^2}\frac{\partial}{\partial y}\left(\tilde{c}^2\frac{\partial\psi}{\partial y}\right) + \omega^2\left(\frac{1}{\tilde{c}^2} - 1\right)\psi\right]. \quad (6)$$

The equation (6) and the impedance boundary condition (3) are finite-differenced and the solution is obtained by marching forward in the *x* direction. Sandy soil is taken to be the ground surface type beyond the freeway with $\sigma = 4\text{x}10^5$ Pa s m^{-2} and we assume the ground is completely flat to concentrate strictly on atmospheric effects in this study.

The radiation condition (2) is dealt with numerically by a buffer zone[14,36,37] occupying approximately the upper one third of the grid domain, $y_{att} < y < y_{max}$, where the effective sound speed $\tilde{c}$ in (6) is replaced by

$$\bar{c}(y) = \tilde{c}(y)\left[1 + iA\left(\frac{y - y_{att}}{y_{\max} - y_{att}}\right)^3\right]^{-1}$$

Here, A is a real parameter that can be optimized for each frequency component. To ensure the effectiveness of the buffer zone, the initial pressure profile obtained from the near-field Green's function method $p_{ini}(y)$ must also be smoothly reduced to zero within the buffer zone to prevent spurious reflections from the truncated top of the grid domain. Thus,

$$\psi(x_{edge}, y) = p_{ini} \exp\left(-\frac{B\omega^2}{2}\left(\frac{y - y_{att}}{y_{\max} - y_{att}}\right)^2 - i\omega x_{edge}\right)$$

where $1 \le B \le 4$ is another optimized parameter dependent on frequency.

Effects of atmospheric absorption are incorporated following the method outlined in Salomons[5] §B.5 by applying a constant attenuation rate in dB m^{-1} to each frequency band at 1 m agl before summing to form the L_{eq} versus range plots. This method follows the International Standard ISO 9613-1:1993(E). In doing so, it was necessary to approximate a value for the relative humidity, which was only measured with the balloon-tethersonde system during the October measurements. We used a value of 20 percent relative humidity, 20˚C, and atmospheric pressure of 101.325 kPa.

IV. CHOSEN TEST CASES AND MODELLING PARAMETERS

The field experiments yielded large amounts of meteorological and sound data. Three representative cases were selected for sound transmission modeling based on the velocity profiles and stratification. Temperature and crosswind profiles above 131 ft (40 m) were obtained from the SODAR/RASS measurements in 32.8 ft (10 m) increments, whereas data at lower altitudes were gleaned from the sonic anemometer readings (which were located only at fixed locations). The meteorological profiles are time-averaged over a period of 20 minutes. To obtain the surface-layer velocity profile for an unstable convective boundary layer (<200 ft or 60 m), theoretical curves of the Monin-Obukhov (MO) similarity theory are then fitted to the sonic data. The MO theory suggests that near the ground both vertical temperature and velocity gradients have the form

$$\frac{\partial \bar{\varsigma}}{\partial y} \sim A_{\bar{\varsigma}}\left(1 - B_{\bar{\varsigma}}\right)^{2/3} y^{-4/3} \text{for } \bar{\varsigma} = U_0(y), T(y). \tag{7}$$

where $A_{\bar{\varsigma}}$ and $B_{\bar{\varsigma}}$ are parameters fitted to the data.[38] Since $\frac{\partial \bar{\varsigma}}{\partial y}$ diverges like $y^{-4/3}$ as $y \to 0$, the chosen temperature profile is made linear near the ground so that $T(y) \sim A\, y + B$ and the velocity takes instead a standard logarithmic form, $U_0(y) \sim A \log(z/z^*)$, where z^* is the aerodynamic roughness length (which is acceptable below a distance of MO length scale, as the dominant term therein is shear generated turbulence). Above approximately 200 ft (60 m), the fitted curve smoothly transitions into the SODAR-RASS data. If the useful range of data from the SODAR/RASS is less than 984 ft (300 m), the theoretical curve is held constant at the last entry from the SODAR-RASS. Measurements and theoretical profiles for the three chosen cases are shown in Figures 8 to 10.

Case A: Nov 7, 2006 (Loop 202) 10:40 to 11:00am

This case has wind shear at very high altitudes, but with very little temperature stratification. Plots of experimental and theoretical profiles for temperature and crosswind velocity are shown in Figure 8. Note that in Case A, the SODAR-RASS data was usable up to 820 ft (250 m), compared to 656 ft (200 m) for other cases.

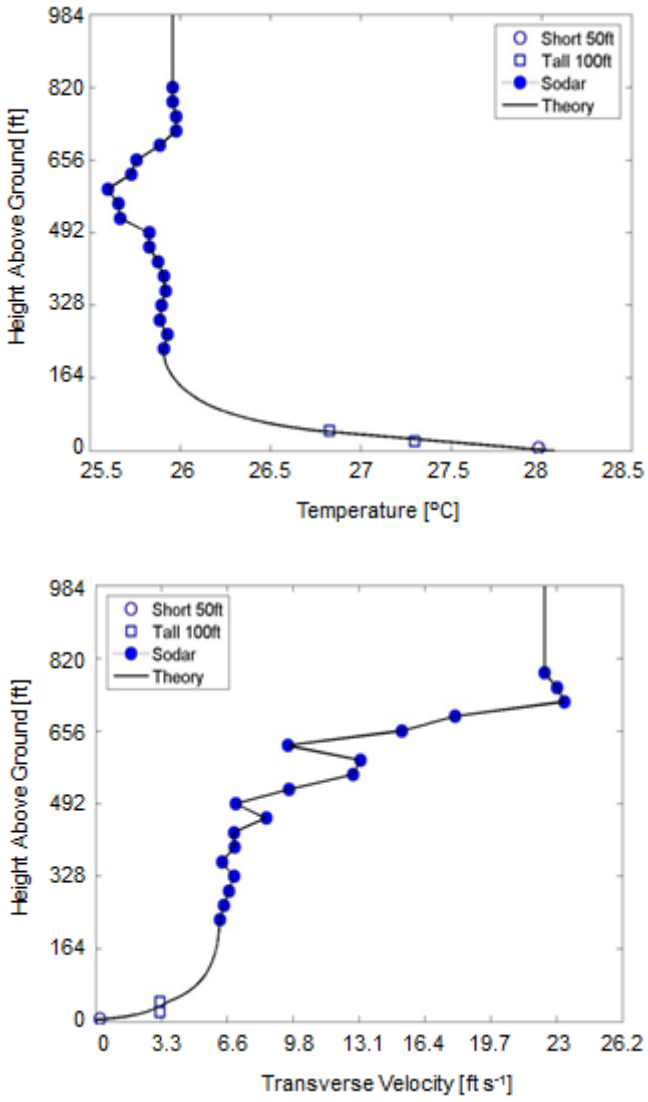

Figure 8. Case A: Temperature and crosswind (to the freeway) data with fitted theoretical profiles. Open circles are data from the sonic anemometers 50 ft from the center of the near lane, open squares are from anemometers 100 ft from the near lane, solid circles are from the SODAR-RASS, and the solid line is the theoretical curve entered into our model.

Case B: Nov 7, 2006 (Loop 202) 7:40 to 8:00am

This case is stratified with shear flow. Plots of experimental and theoretical profiles for temperature and crosswind velocity are shown in Figure 9.

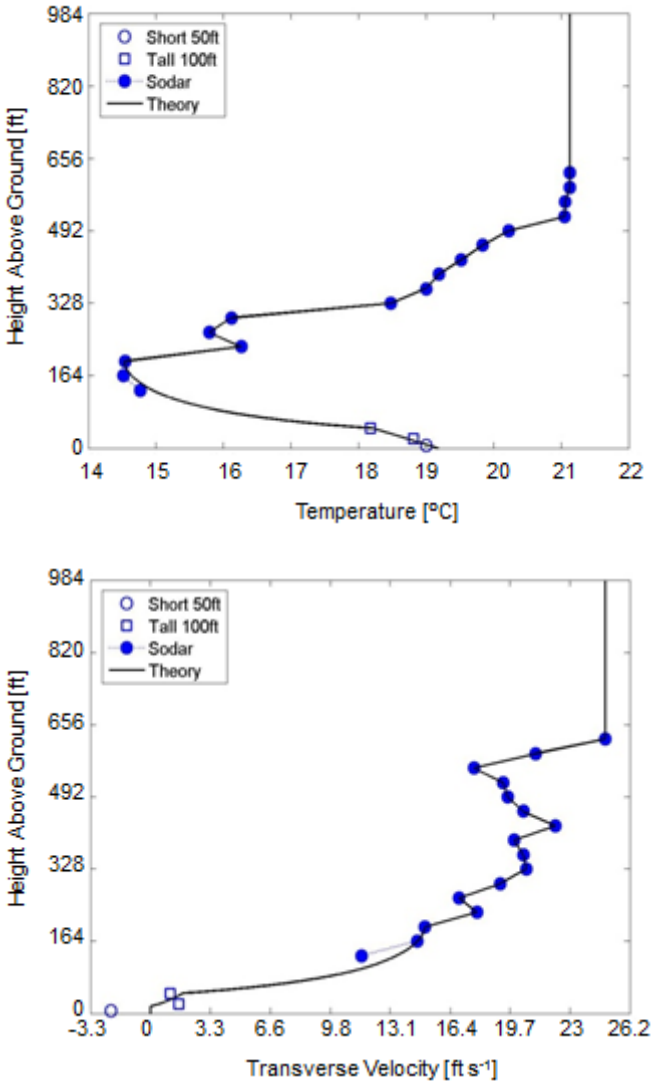

Figure 9. Case B: Temperature and crosswind (to the freeway) data with fitted theoretical profiles. Open circles are data from the sonic anemometers 50 ft from the center of the near lane, open squares are anemometers 100 ft from the near lane, solid circles are from the SODAR-RASS, and the solid line is the theoretical curve entered into our model.

Case C: Nov 8, 2006 (Loop 202) 7:40 to 8:00am

This case is strongly stratified with a sharp change in temperature at approximately 394 ft (120 m) above the ground and a crosswind jet at approximately 164 ft (50 m) above the ground. Plots of experimental and theoretical profiles for temperature and crosswind velocity are shown in Figure 10.

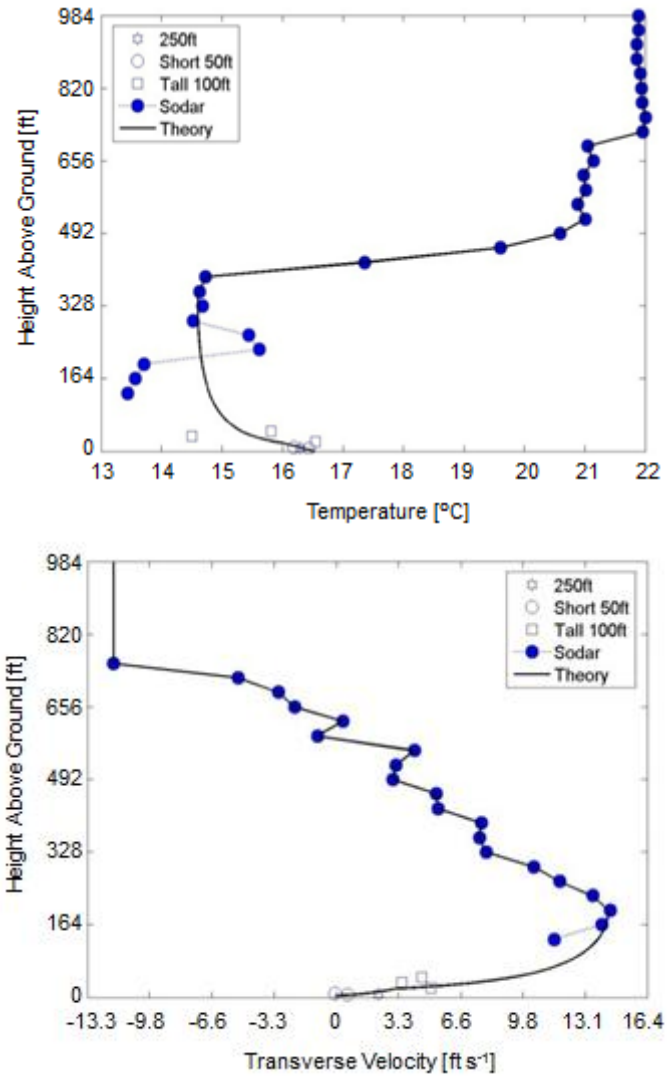

Figure 10. Case C: Temperature and crosswind (to the freeway) data with fitted theoretical profiles. Open circles are data from the sonic anemometers 50 ft from the center of the near lane, open squares are anemometers 100 ft from the near lane, solid circles are from the SODAR-RASS, and the solid line is the theoretical curve entered into our model.

V. ANALYSIS OF TRAFFIC SPECTRA TAKEN BY NOISE METERS

The overall acoustic source field we are attempting to replicate consists of a six-lane highway (three lanes in each direction) with multiple moving sound sources that vary according to their speed, the traffic density, and the vehicular type. Without knowledge of the exact acoustic signature of every car and truck, a number of severe but unavoidable assumptions needed to be made about the nature of the sound sources. We emphasize here that the focus of this paper is on the meteorological aspect of noise transmission from freeways, as opposed to understanding the composition of sound sources emitted, and the results are expected to give useful information on the effects of temperature stratification and wind shear on the noise propagation.

The sound data consists of five-minute time-averaged one-third octave data from three sound meters placed close to the highway. We do not have information on sound generated from separate lanes of traffic and the frequency output of different vehicle types traveling at different speeds. However, Figure 11 shows the difference between the five-minute averaged dBA level taken from the sound meter located 50 ft (15.2 m) away from the center of the nearest travel lane and 5 ft (1.5 m) above the ground and that located 100 ft (30.5 m) away from the center of the nearest travel lanes and 5 ft (1.5 m) above the ground on one of the nearest travel lane and 5 ft (1.5 m) above the ground and that located 100 ft (30.5 m) away from the center of the nearest travel lane and 5 ft (1.5 m) above the ground on one particular day of field experiments. This clearly shows a geometric attenuation of 3dB as the distance from the source doubles, providing some justification to the assumption that the freeway can be treated as series of line sources.

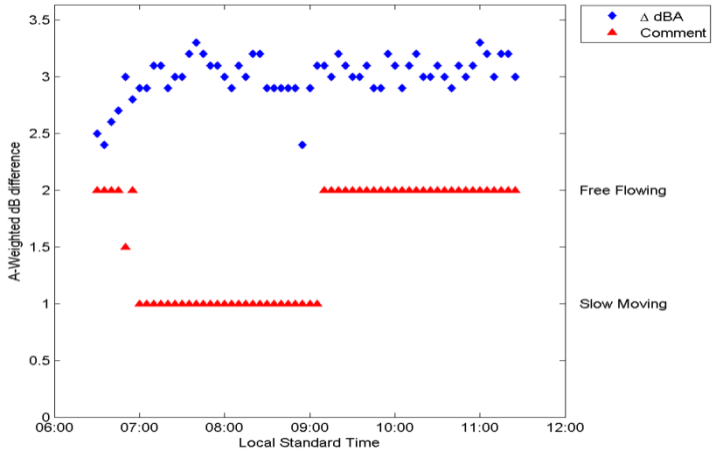

Figure 11. The difference in overall A-weighted sound level measured between the sound meter located 50 ft (15.2 m) from the center of the freeway's nearest lane at a height of 5 ft (1.5 m) and the sound meter located 100 ft (30.5 m) from the near lane at a height of 5 ft (1.5 m). The triangles merely display an indication of the traffic conditions at the time (either free flowing or slow moving). A decrease of 3dB with a doubling of distance corresponds to what is expected for a line source as $P_{line} \sim 1/r$ in a neutral atmosphere.

We assume that over the ranges in question (up to 1965 ft (600 m)), the sound field in a neutral atmosphere (i.e., constant temperature with zero mean flow) continues to evolve in a two-dimensional fashion, with a geometric attenuation of 3 dB as the distance doubles from the freeway. In our model, the traffic noise is approximated as a series of monofrequency coherent line sources positioned vertically above the nearest travel lane of the freeway (see Figure 12).

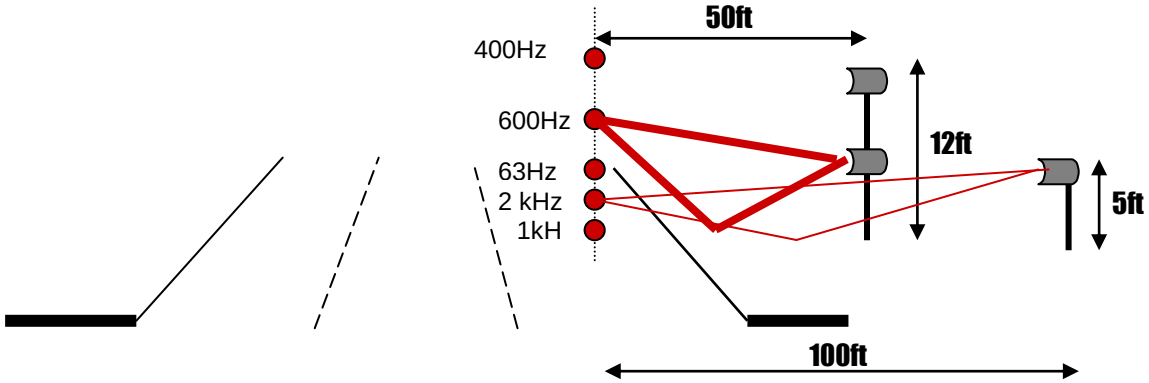

Figure 12. A schematic showing sound rays emanating from a series of example mono-frequency coherent sound sources positioned at the center of the near lane of the freeway.

The strength and effective height of these virtual sources are unknowns that must be determined from the one-third octave data obtained from the three (or four) sound meters. As the sound meters are positioned relatively close to the source, the influence of meteorological conditions is regarded as negligible over the range up to the farthest sound meter and a neutral atmosphere is therefore assumed in the near field. This enables the unknown line source parameters to be determined by using the Green's function model for acoustic propagation from a line source above an impedance plane as detailed in Section III. As mentioned before, the impedances chosen are taken from Attenborough[6] as $\sigma = 3\text{x}10^7$ Pa s m^{-2} for the asphalt and $\sigma = 4\text{x}10^5$ Pa s m^{-2} for the sandy soil. Due to a lack of exact knowledge of the highway and surrounding surface topography, the surface is assumed to be asphalt out to a range of 50 ft from the virtual line sources with sandy soil beyond, as shown in Figure 13. Repeating the calculation for other impedances suggests that neither the representation of asphalt as a hard wall ($Z = \infty$) nor varying sandy soil impedance between $2\text{x}10^5$to $6\text{x}10^5$ Pa s m^{-2} change the results significantly.

For a given one-third octave interval, the height of a representative line source can be calculated by replicating the differences between the dBA values recorded by the three sound meters. This is done by varying the source height to minimize a norm based on the sum of the absolute errors between the differences obtained by the Green's function model and the recorded differences. The range of possible source heights is restricted to less than 4 m and the lowest height where the error norm attains a local minimum and takes an absolute value less than 2dB–3dB is selected. The source heights used for Cases A through C are shown in Figure 14. Note that there is very good agreement on the source heights obtained in each case for the higher frequencies (using data taken on different days at different times). Larger discrepancies for the lower frequencies can be explained as the dBA difference errors do not vary that much with height due to the large wavelengths. This also means that the accuracy

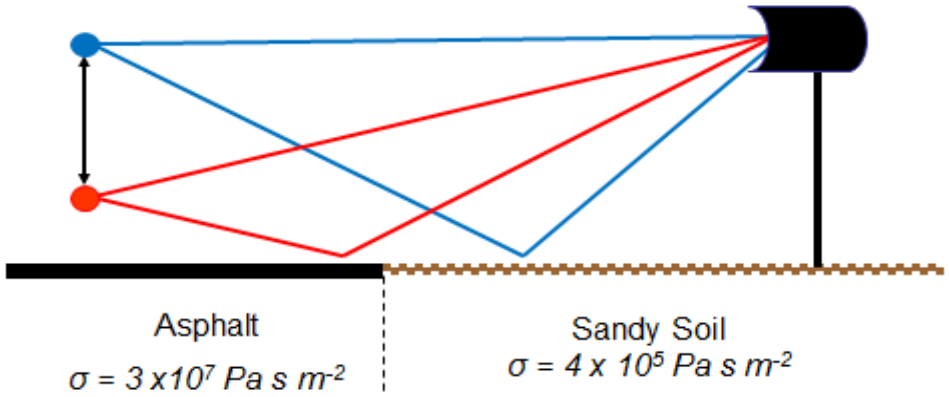

Figure 13. Schematic demonstrating the calculation of virtual source heights for each one-third octave frequency component. Shown are two example source heights (blue and red) along with the direct and once-reflected rays that superimpose upon reaching the sound meter. Ground impedance boundary conditions change not only amplitude, but also the phase of the reflected ray (see equation 5).

of the source height for lower frequencies is less crucial as it does not significantly alter the sound field. Perhaps the most problematic difficulty in selecting source height for 315Hz–400Hz range, where the norm error at zero height is unacceptably high (possibly 9dB-10dB) but the error norm approaches zero again at source heights of 11.5 ft–14.8 ft (3.5 m–4.5 m); thus heights of this order are chosen.

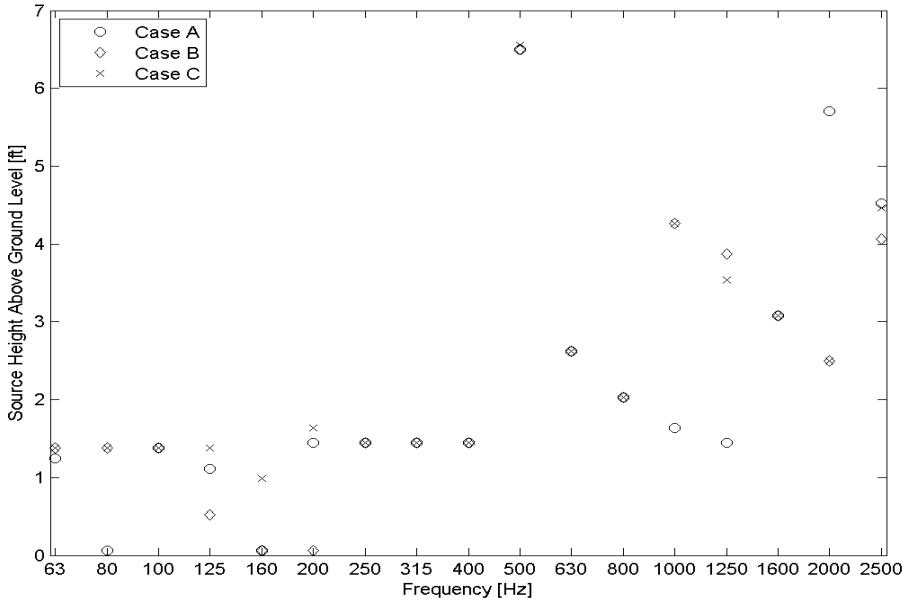

Figure 14. Source heights for Loop 202 cases obtained by minimizing an error norm based on dB differences between sound meters for Case A (circles), Case B (diamonds), and Case C (crosses).

Following the determination of source heights, it is relatively straightforward to use the Green's function near-field model to obtain the A-weighted source strengths, and these are given for Cases A through C in Figure 15. Note the good agreement in the source strength profile across the frequency ranges 63Hz–2.5kHz for the three cases. The sound signature is almost identical for Cases B and C, both taken at the same time during rush hour on consecutive days, whereas Case A has lower sound levels particularly in the 100Hz–200Hz and 800Hz–2kHz band, possibly due to the lower traffic levels occurring in the late morning.

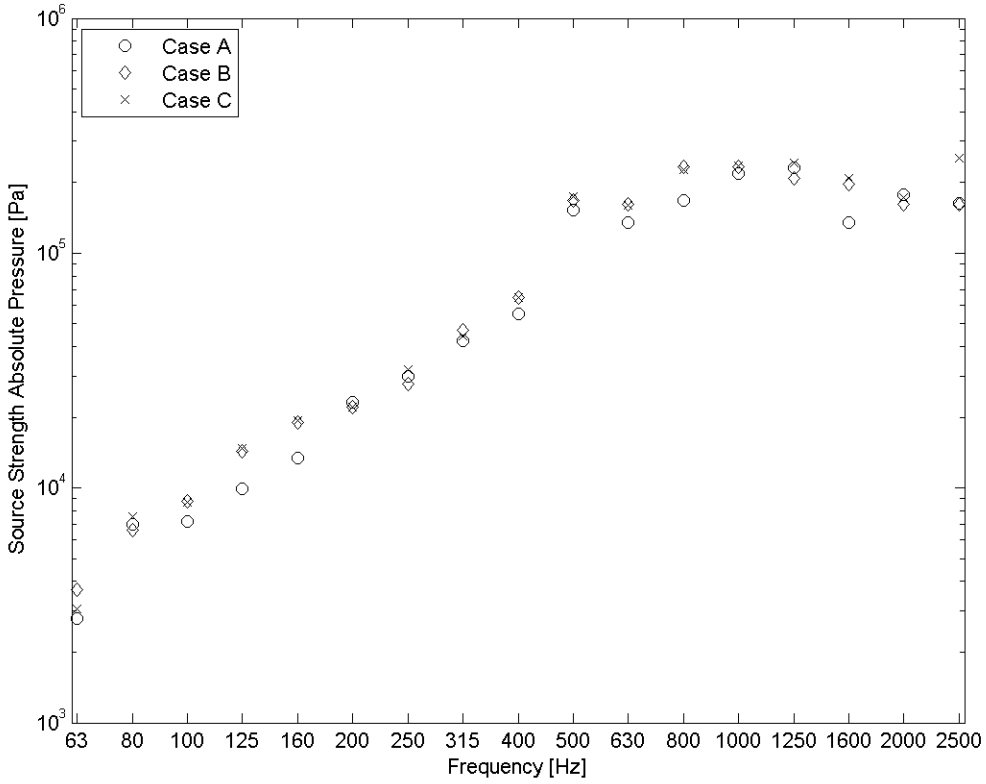

Figure 15. Source strengths for Loop 202 cases obtained by minimizing an error norm based on dB differences between the sound meters for Case A (circles), Case B (diamonds), and Case C (crosses).

VI. CONSTRUCTION OF L_{EQ} PLOTS

In each chosen case, the model is run for each frequency component, based on the central frequency of the one-third octave band, with and without the influence of meteorological effects for comparison. For efficiency, the frequency range of the computation is reduced from spanning the entire range of frequency bands from 25Hz–20kHz to only include those bands between 63Hz and 2.5kHz (17 components in all). Such a restriction produces an error of less than 0.2 percent in terms of the final overall sound pressure level when compared to the actual values measured by the sound meters.

The spatial A-weighted sound pressure level distribution for each frequency component is resolved by the PE model on a grid of size and spacing dependent on the wavelength (based on a usual 10 grid points per wavelength). These results are subsequently interpolated onto a grid of 3.28 ft (1 m) spacing with a range of 0 ft–1965 ft (0 m–600 m) horizontally and 0 ft–984 ft (0 m–300 m) vertically. Then at each grid point the A-weighted frequency contributions $L_A(f_n)\,(x,y)$ are combined to produce the overall L_{eq} sound pressure level by the formula[5]

$$L_{eq} = 10\log_{10}\sum_{n=1}^{17} 10^{L_A(f_n)/10}$$

with

$$f_n = \begin{Bmatrix} 63 & 125 & 250 & 500 & 1000 & 2000 \\ 80 & 160 & 315 & 630 & 1250 & 2500 \\ 100 & 200 & 400 & 800 & 1600 & \end{Bmatrix} \text{ [Hz]}$$

Results of the spatial sound pressure levels are presented in Figures 16 to 18 for Case A, Figures 19 to 21 for Case B, and Figures 22 to 24 for Case C. Each result presents the equivalent spatial sound field obtained in a neutral atmosphere directly above the resolved spatial sound field when the temperature and crosswind velocity effects are included. Note that the downwind side of the freeway is always shown and the vertical range displayed is only up to 65.6 ft (20 m) agl. It is clear from these figures that the overall impact of the meteorological effects is significant in all three cases examined. Indeed, significantly higher noise levels are predicted downwind near ground level for all cases. For guidance, FHWA's noise abatement criteria threshold of 67dBA is shown as a thick contour line on the spatial contour plots of L_{eq} and by a gray area on the sound pressure level range plots at 3.28 ft (1 m) above the ground. Below, each case is examined in more detail.

The meteorological effects are weakest for Case A, with very little temperature stratification and a crosswind on the order of 6.6 ft s^{-1} (2 m s^{-1}) persisting from about

98 ft (30 m) to around 492 ft (150 m) in altitude. However, Figure 16 clearly shows how the crosswind shear flow present up to 98 ft (30 m) above the surface focuses sound into a thin layer of around 7 ft to 16 ft (2 m to 5 m) in height, where the sound intensity is raised by roughly 15dB.

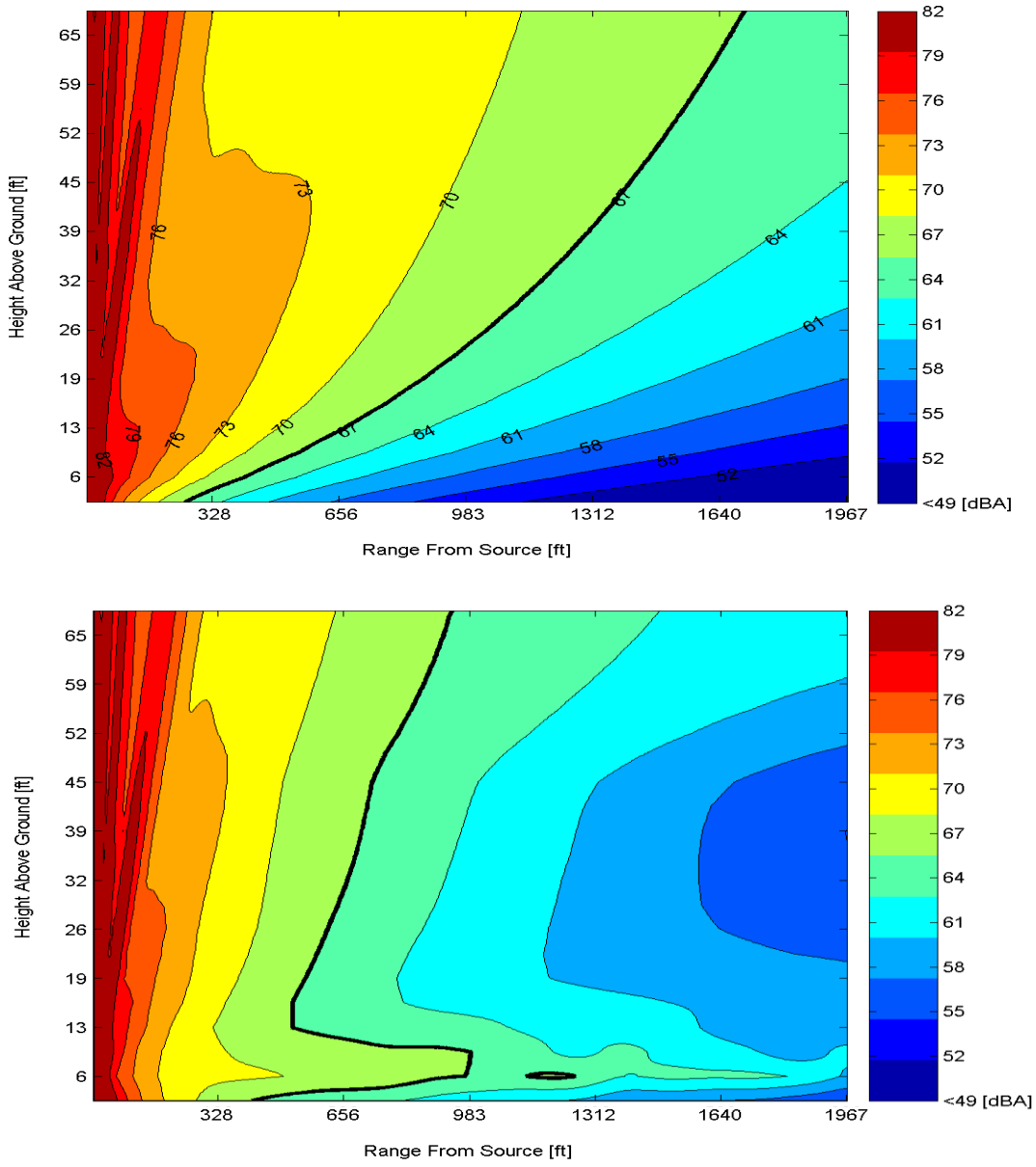

Figure 16. Case A: A-weighted sound pressure level contours without meteorological effects (top) and with meteorological effects (bottom). Each contour line represents a change of 3dBA.

As a result, the sound level close to the ground does not fall below 67dBA until a horizontal distance of 1637 ft (500 m) from the freeway is reached, as opposed to approximately 328 ft (100 m) predicted for a neutral atmosphere (see Figure 17).

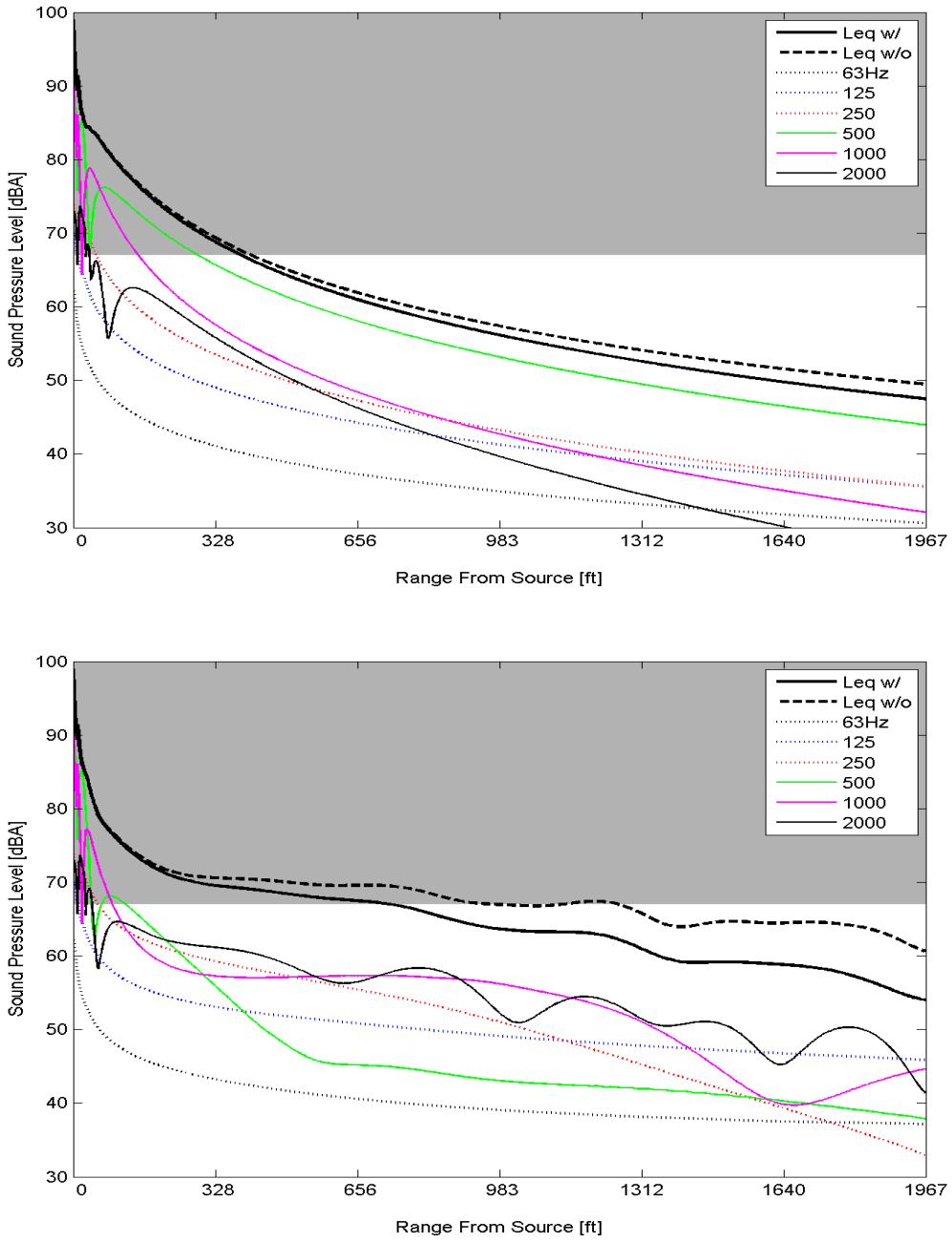

Figure 17. Case A: Overall A-weighted sound pressure level and frequency components at 1 m above the ground without meteorological effects (top) and with meteorological effects (bottom). The gray marks the area over 67dB level. Only a few frequency bands are shown for clarity.

An examination of Figure 18 of the impact of the meteorological effects on individual frequency components reveals that the frequency band 1kHz–2kHz remains the most intense out to the far field.

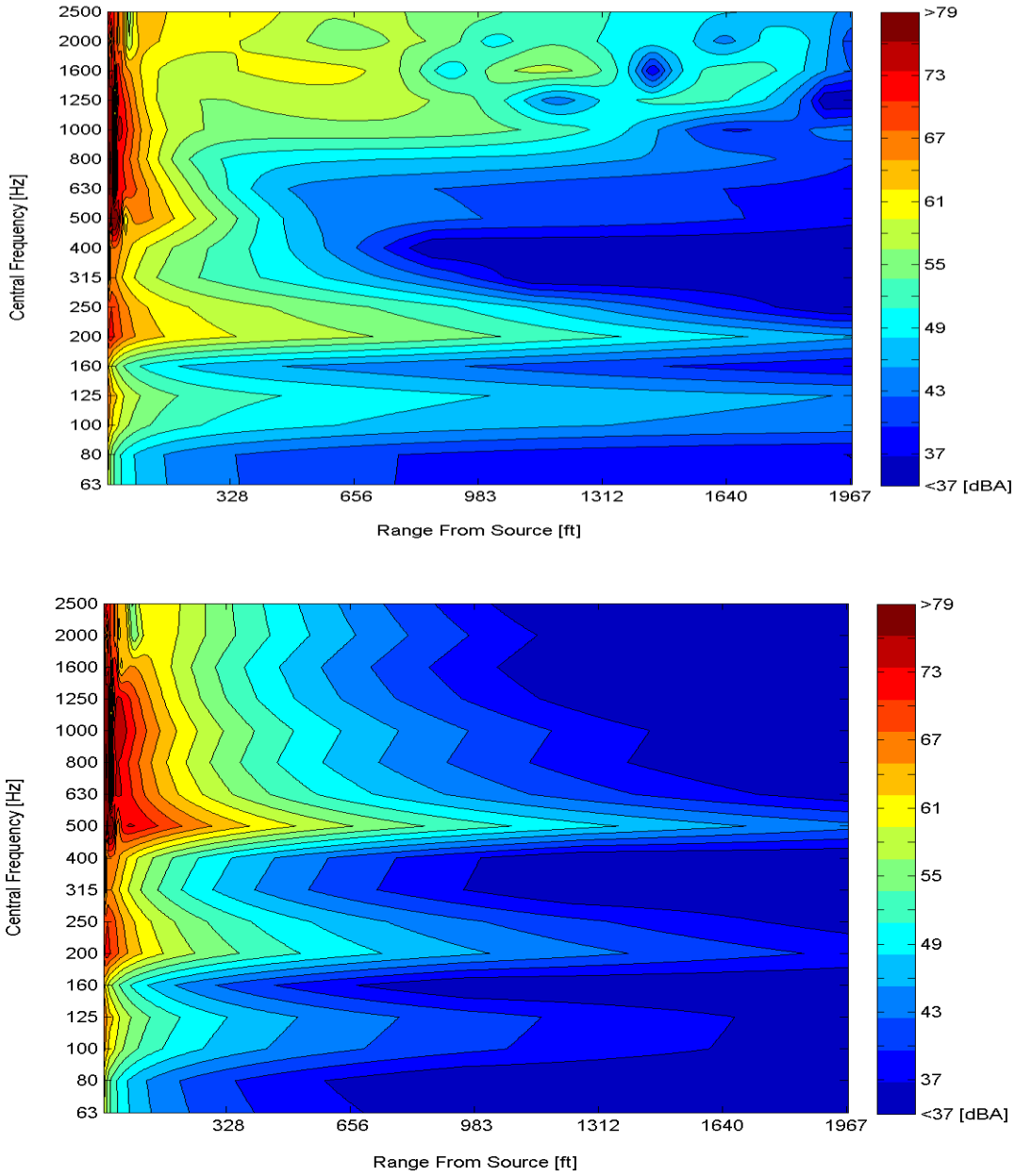

Figure 18. Case A: Contours of A-weighted sound pressure level for each frequency component for neutral (top) and meteorological (bottom). Each contour line represents a change of 3dBA.

Case B occurred during the rush-hour traffic on Loop 202 with a stronger wind shear resulting in speeds of approximately 19fts^{-1} (6ms^{-1}) at approximately 200 ft (60 m) agl. More severe temperature gradients are observed, with the temperature falling 5^{o}C with increasing altitude before rising back to its ground level value at an altitude of approximately 330 ft

(100 m). The competition between the near-ground negative temperature gradient and positive wind shear means that overall near-ground sound levels fall in a similar fashion as in neutral atmospheric conditions over the first 656 ft (200 m) from the freeway. However, the refractive effects due to wind shear and the evolution to a temperature inversion at higher altitudes leads to sound rays being refracted back towards the ground from above and sound focusing at around 1637 ft (500 m) from the freeway. Indeed, Figures 19 and 20 indicate that the A-weighted sound pressure level starts to exceed the 67dBA threshold close to the ground at a range of 1637 ft (500 m), before continuing to exceed 67dBA beyond the calculation domain.

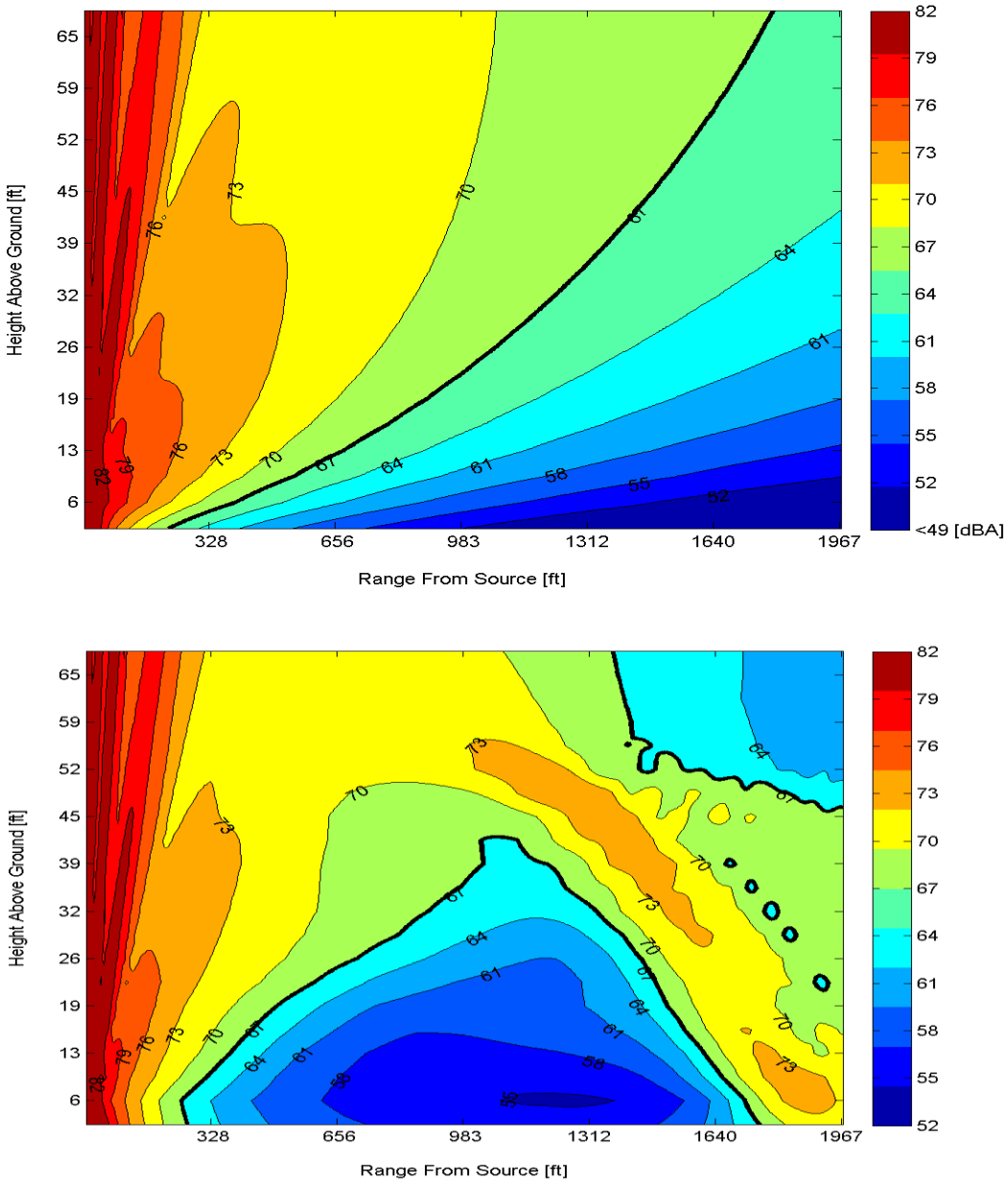

Figure 19. Case B: A-weighted sound pressure level contours without meteorological effects (top) and with meteorological effects (bottom). Each contour line represents a change of 3dBA.

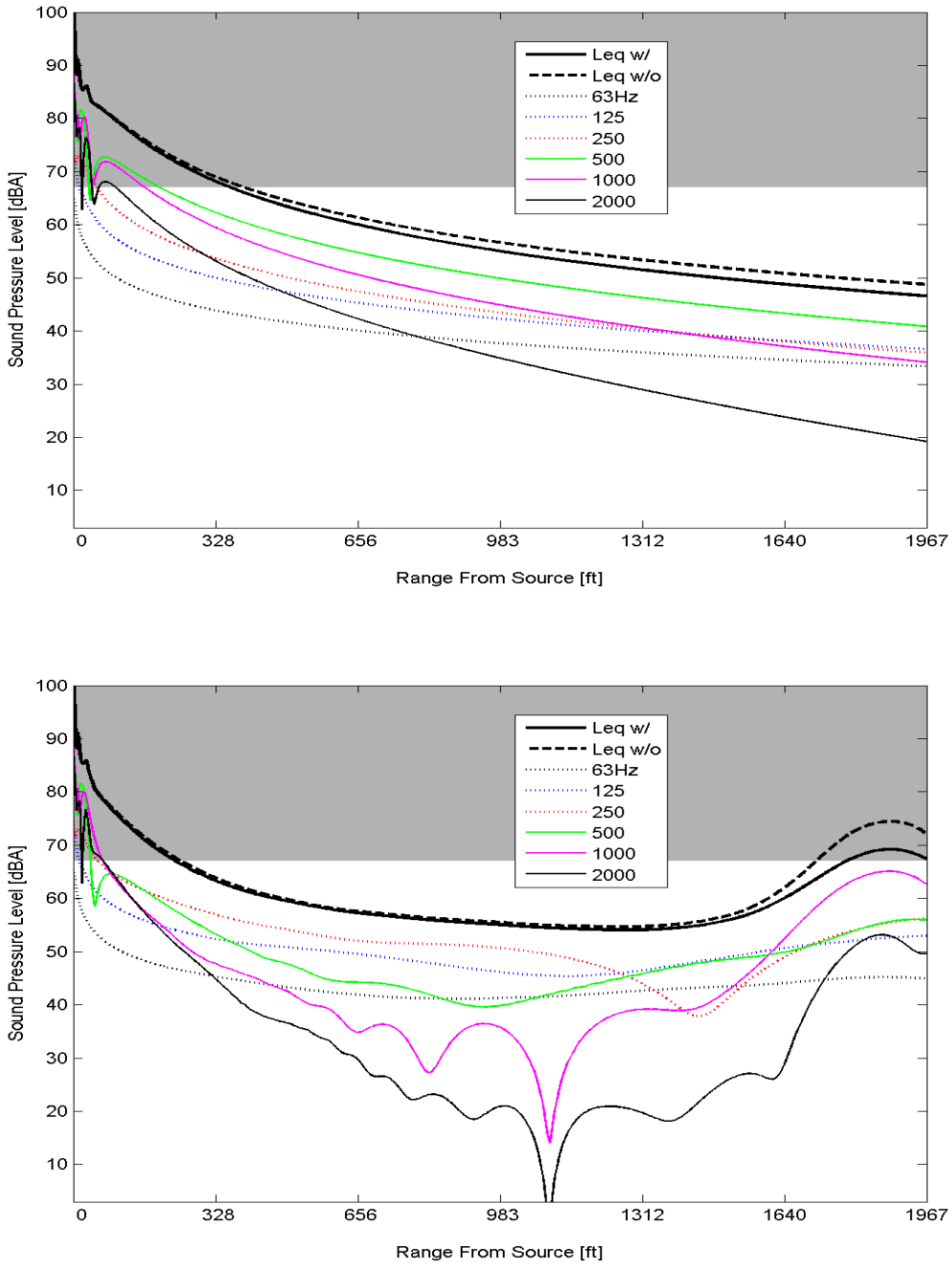

Figure 20. Case B: Overall A-weighted sound pressure level and frequency components at 1 m above the ground without meteorological effects (top) and with meteorological effects (bottom). The gray marks the area over 67dBA level.

Similar to the previous case, the frequency range 1kHz–1.25kHz is particularly influenced and focused most intensely by a combination of wind shear and temperature gradients (Figure 21), although all frequency ranges appear to be subjected to some degree of focusing

at the 1637 ft (500 m) range. The spatial contours in Figure 19 strongly suggest that this case might be a typical example of excessive sound levels occurring far from the freeway, which are unlikely to be abated by the use of a sound barrier.

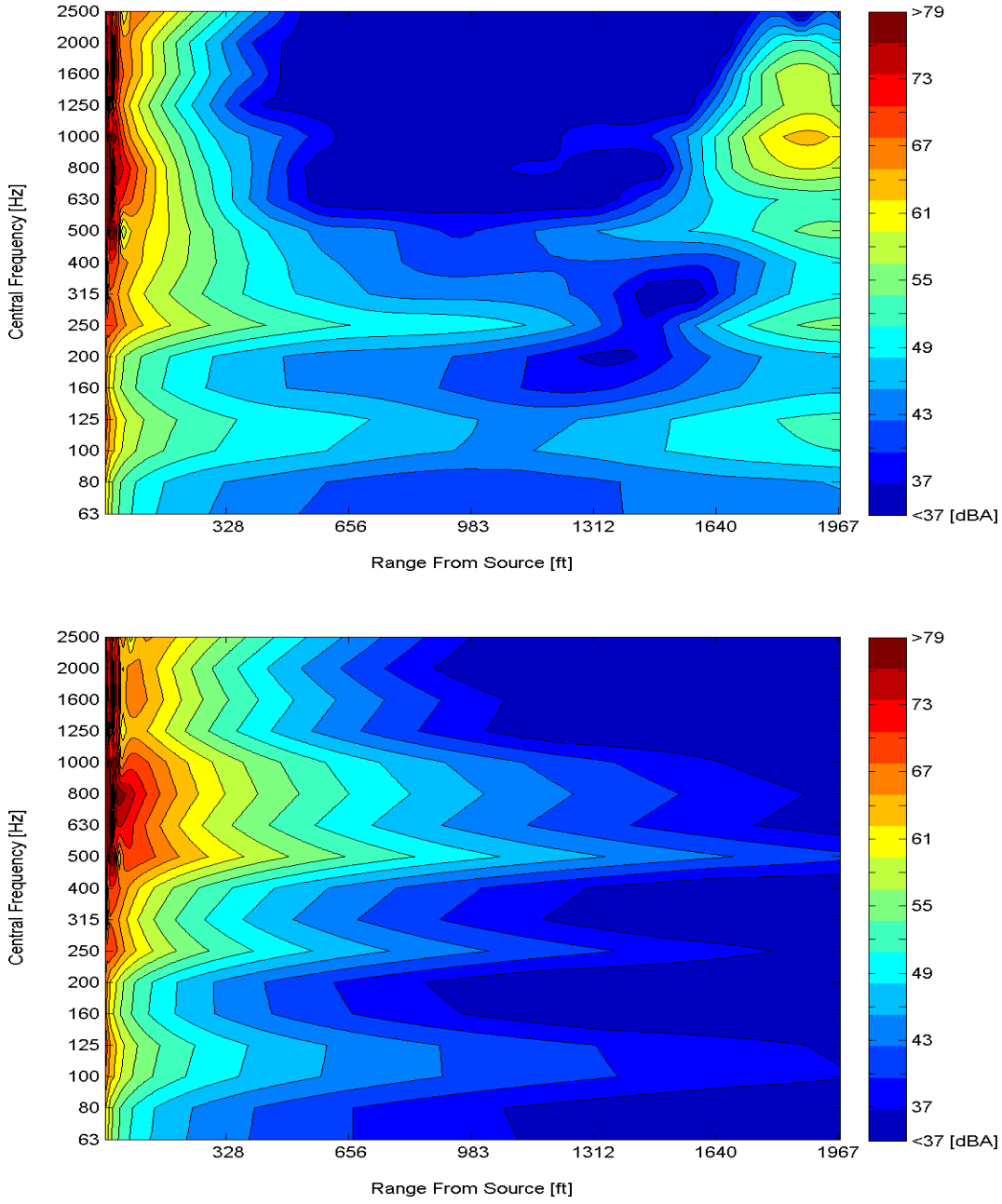

Figure 21. Case B: Contours of A-weighted sound pressure level for each frequency component. Each contour line represents a change of 3dBA.

Case C is also taken during rush-hour traffic and has the most severely changing meteorological profiles, being strongly stratified and having a crosswind jet peaking at 4ms^{-1} at a height of 50 m above the ground. Figures 22 to 25 show a concentration of sound rays and

pockets of constructive and destructive interference between the rays in a roughly 4m-wide layer close to the ground, particularly beyond the 300 m range. As a result, the combined effect of wind shear with a mild negative temperature gradient close to the ground leads to the near-ground sound pressure level persisting in excess of the 67dBA threshold for up to nearly 600 m (approximately 1/3 mile) away from the freeway. The dominant frequencies responsible once again appear to be 1.25 kHz and 1.6 kHz with other neighboring frequencies also being strongly influenced by the meteorological conditions. In addition, sound in the frequency range 125Hz–160Hz appears to be focused to lesser extent in the 500 m–600 m (1639–1967 ft) range.

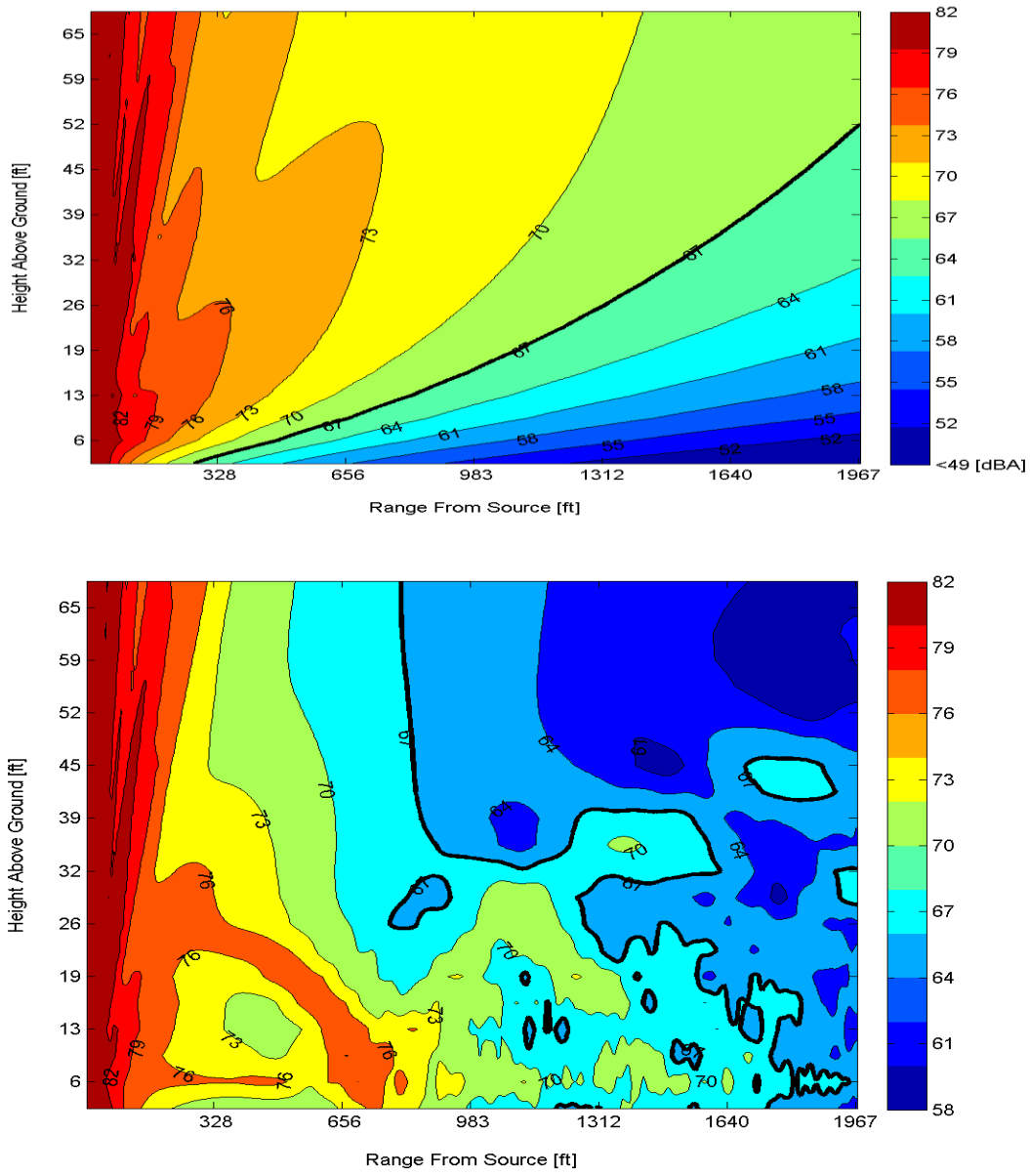

Figure 22. Case C: A-weighted sound pressure level contour without meteorological effects (top) and with meteorological effects (bottom). Each contour line represents a change of 3dBA.

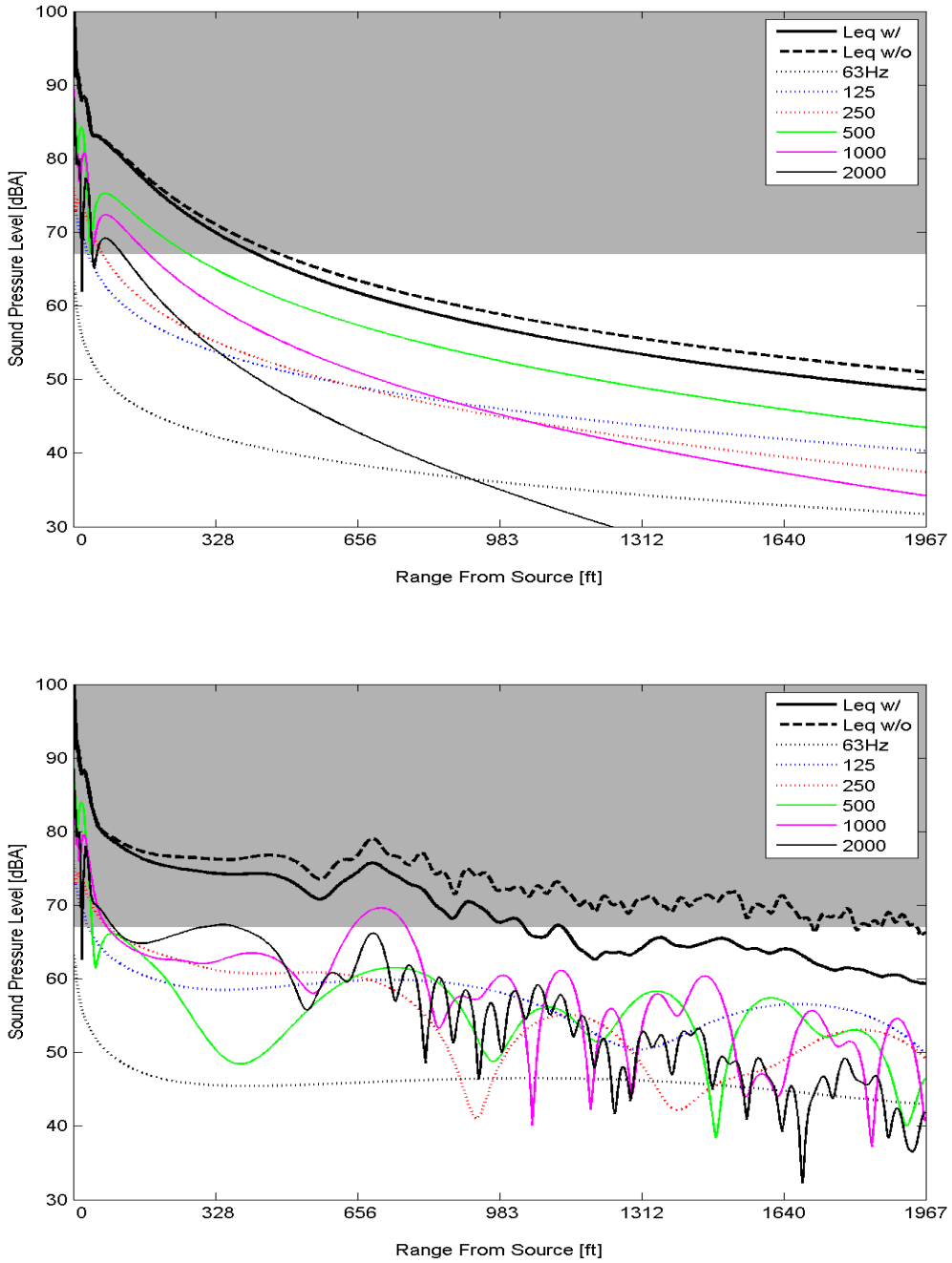

Figure 23. Case C: Overall A-weighted sound pressure level and frequency components at 1 m above the ground without meteorological effects (top) and with meteorological effects (bottom). The gray marks the area over 67dB level.

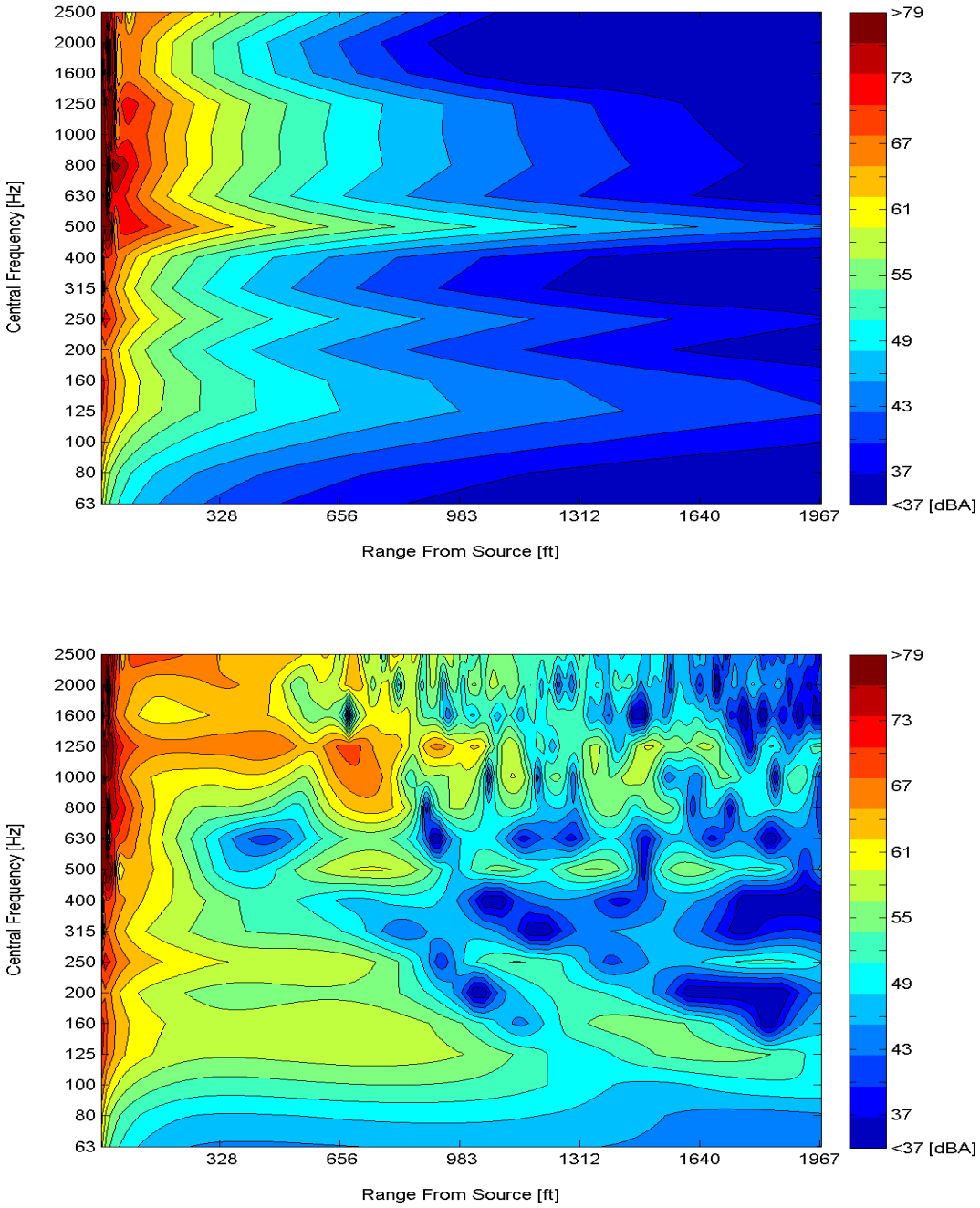

Figure 24. Case C: Contours of A-weighted sound pressure level for each frequency component. Each contour line represents a change of 3dBA.

VII. CONCLUSIONS/ FURTHER COMMENTS

This work represents an initial combined experimental and theoretical study into the impact of meteorological conditions on the propagation of traffic noise from a freeway corridor. The principal conclusions of the study are as follows:

(i) Traffic noise models used to assess environmental noise impacts on nearby communities must incorporate expected meteorological conditions that occur in that location. Noise measurements taken under different meteorological conditions cannot be directly compared to obtain information on the source, unless corrections are made for differing meteorology. This is particular important for the case of ARFC concerned in this study, in that the reduction of the effectiveness of the pavement in use is deduced via measurements made over certain periods of different years. Without corrections for the effects of meteorology, the validity of such assessments is questionable and corrections based on near field data are recommended to transform the data to some standard conditions.

(ii) The combined Green's function and PE model developed as a part of this study has shown its capabilities in taking meteorological data and near-field sound measurements to generate a spatial map of the predicted noise levels. The model also enables analyses of individual frequency components (e.g., as in Figures 17 and 18 for Case A), and the model results show that the frequency range 1kHz–2kHz is the most significantly influenced by meteorological conditions and thus provide the principal contribution to far-field traffic noise levels; this result, however, awaits experimental confirmation. If such evidence arises, mitigation strategies targeting this frequency band would be the most effective in preventing excessive noise levels at large distances from the freeway corridor.

(iii) This work represents the initiation of further collaborative investigations between ADOT and EFD-ASU that are focused on assessing the effectiveness of noise mitigation strategies, in particular comparing the efficacy of different noise barriers (e.g., absorptive barrier surfaces, land-use control, traffic-management measures, vegetative barrier, ARFC). Future experiments and development of the theoretical models will require (a) assessing the effects of turbulence, (b) improved field trials with more sound meters to give further spatial sound information and meteorological data, and (c) an examination of terrain effects in the surrounding areas, which is needed for better accuracy of freeway acoustic work. More accurate knowledge of the sound field and types of sources is also required.

(iv) Another important issue with physical noise barriers is the flow field distortion surrounding them. This may greatly influence source characteristics for far-field noise, in addition to direct influence on near-field characteristics. Inclusion of such effects needs to be done using complex high-resolution flow models that account for fine-scale features. These models can be nested in a meso-scale weather prediction model, as was demonstrated by Fernando et al.[12] A model of the genre has been developed by the EFD group,[39] and combining the new acoustic model developed here with such a nested model will be the most sophisticated methodology that can be proposed for future highway acoustic evaluation studies. Figure 25 shows an

example of a calculation conducted to illustrate the effects of nearby buildings and a small topographic feature (butte) on an approaching flow field for neutral conditions. Under convective or stable conditions, the flow field is expected to be more complex as demonstrated in the figure; for example, it has flow separation, reattachment, and recirculation regions as well intense turbulence production in these highly sheared areas. These models, however, will be computer intensive and hence collaboration with a high-performance computing cluster is recommended. If noise barriers are present on either side of the freeway, then back scattering of acoustic waves needs to be taken into account.

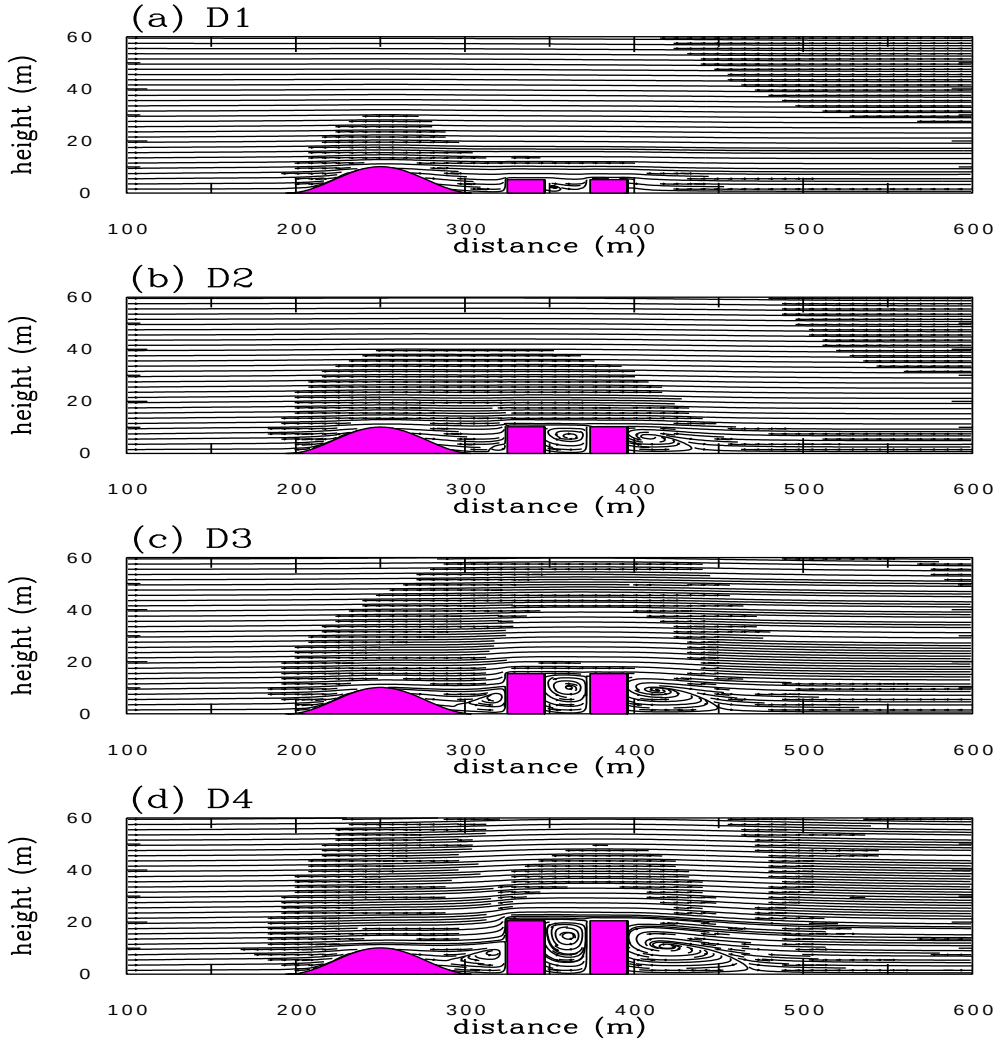

Figure 25. The distortion of flow by a set of barriers, as computed by a high-resolution computational fluid dynamics code that uses Large-Eddy Simulation method. Such a model can be nested with a meteorological model on a high-performance computational platform to assess acoustic behavior in built-up areas. Different building heights are illustrated. Similarly, a noise wall can be included in the simulation.

(v) It is expected that ADOT will use the model developed or a further improved version thereof for a direct comparison of the effectiveness of barriers and ARFC in the near future. As mentioned, accounting for meteorological conditions is imperative in further field trials.

(vi) Future field experiments should include far-field monitoring as well as collecting more high-resolution meteorological data. The former will help evaluation of the model developed in this study for far-field noise predictions, and the latter will help to determine the resolution to which the meteorological data must be collected for making reasonable practical predictions. The present investigation was limited to near-field sound, as well as general meteorological conditions surrounding a freeway without any noise walls, which is an acceptable first step.

REFERENCES

1. Goines, L. and L. Hagler. "Noise pollution: A modern plague." *Southern Medical Journal* 100(3): 287-294, March 2007.
2. Tapia Granados, J. A. "Reducing automobile traffic: An urgent policy for health promotion." *Revista Panamericana de Salud Publica* 3(4):227-241, 1998.
3. Ward, L. M. and P. Suedfeld. "Human response to highway noise." *Environmental Research* 6(3): 306-326, 1973.
4. Forman, R. T. T. "Estimate of the area affected ecologically by the road system in the United States." *Conservation Biology* 14(1): 31-35, 2000.
5. Salomons, E. M. *Computational Atmospheric Acoustics*. Kluwer Academic Publishers, 2001.
6. Attenborough, K., K.M. Li, and K. Horoshenkov. *Predicting Outdoor Sound*. Taylor and Francis, 2007.
7. Steele, C. "A critical review of some traffic noise prediction models." *Applied Acoustics* 62(3): 271-287, 2001.
8. Lihoreau, B., B. Gauvreau, M. Berengier, P. Blanc-Benon, and I. Calmet. "Outdoor sound propagation modeling in realistic environments: Application of coupled parabolic and atmospheric models." *The Journal of the Acoustical Society of America* 120: 110-119, 2006.
9. Wayson, R. L., J. M. MacDonald, R. D. Eaglin, and B. Wendling. "Simulation approach to transport noise modeling." *Transportation Research Record* 1601: 64-70, 1995.
10. Chambers, J., H. Saurenman, R. Bronsdon, L. Sutherland, K. Gilbert, R. Waxler, and C. Talmadge."Effects of temperature induced inversion conditions on suburban highway noise levels." *ActaAcustica united with Acustica* 92(6): 1060-1070, 2006.
11. Wang, J. X. L. and J. K. Angell. *Air Stagnation Climatology for the United States (1948–1998)*. NOAA/Air Resources Laboratory ATLAS No. 1. United States. National Oceanic and Atmospheric Administration, 1999.
12. Fernando, H. J. S., S. M. Lee, J. Anderson, M. Princevac, E. Pardyjak, and S. Grossman-Clarke. "Urban fluid mechanics: Air circulation and contaminant dispersion in cities." *Journal of Environmental Fluid Mechanics* 1(1): 107-164, 2001.
13. Gilbert, K. E. and M. J. White. "Application of the parabolic equation to sound propagation in a refracting atmosphere." *The Journal of the Acoustical Society of America* 85: 630-637, 1989.
14. West, M., K. Gilbert, and R. Sack. "A tutorial on the parabolic equation (PE) model used for long range sound propagation in the atmosphere." *Applied Acoustics* 37: 31-49, 1992.

15. Gilbert, K. and X. Di. “A fast Green’s function method for one-way sound propagation in the atmosphere.” *The Journal of the Acoustical Society of America* 94: 2343-2352, 1993.

16. Di, X. and K. Gilbert. “The effect of turbulence and irregular terrain on outdoor sound propagation.” in *Proceedings of the 6th International Symposium on Long Range Sound Propagation*, ed. by David I. Havelock, 315-333. Canada National Research Council, 1994.

17. Sack, R. and M. West. “A parabolic equation for sound propagation in two dimensions over any smooth terrain profile: The generalized terrain parabolic equation (gt-pe).” *Applied Acoustics* 45: 113-129, 1995.

18. West, M. and Y. Lam. “Prediction of sound fields in the presence of terrain features which produce a range dependent meteorology using the generalized terrain parabolic equation (gt-pe) model.”*InterNoise 2000 Proceedings*, ed. by Didier Cassereau, 2: 943, Paris: Societe Francaise d’Acousticque, 2000.

19. Wilson, D.K. “A turbulence spectral model for sound propagation in the atmosphere that incorporates shear and buoyancy forcing.” *The Journal of the Acoustical Society of America* 108: 2021-2038, 2000.

20. Wilson, D.K., J.G. Brasseur, and K.E. Gilbert. “Acoustic scattering and the spectrum of atmospheric turbulence” *The Journal of the Acoustical Society of America* 105: 30-34, 1999.

21. Chevret, P., P. Blanc-Benon, and D. Juve. “A numerical model for sound propagation through a turbulent atmosphere near the ground.” *The Journal of the Acoustical Society of America* 100: 3587-3599, 1996.

22. Lee, S., N. Bong, W. Richards, and R. Raspet. “Impedance formulation of the fast field program for acoustic wave propagation in the atmosphere.” *The Journal of the Acoustical Society of America* 79: 628-634, 1986.

23. Franke, S. and G. W. J. Swenson. “Brief tutorial on the fast field program (ffp) as applied to sound propagation in the air.” *Applied Acoustics* 27: 203-215, 1989.

24. West, M., R. Sack, and F. Walkden. “The fast field program (ffp) a second tutorial: Application to long range sound propagation in the atmosphere.” *Applied Acoustics* 33: 199-228, 1991.

25. Wilson, D.K. “Sound field computations in a stratified, moving medium.” *The Journal of the Acoustical Society of America* 94: 400-407, 1993.

26. Nijs, L. and C. Wapenaar. “The influence of wind and temperature gradients on sound propagation, calculated with the two-way wave equation.” *The Journal of the Acoustical Society of America* 87: 1987-1998, 1990.

27. Nijs, L. and C. Wapenaar. “Reply to: Comments on the influence of wind and temperature gradients on sound propagation calculated with the two-way wave equation.” *The Journal of the Acoustical Society of America* 91: 498-500, 1992.

28. Ostashev, V. *Acoustics in a Moving Inhomogeneous Media*. Spon Press, 1997.

29. Ostashev, V., V. Mellert, R. Wandelt, and F. Gerdes. “Propagation of sound in a turbulent medium: I. – Plane waves.” *The Journal of the Acoustical Society of America* 102: 2561-2570, 1997.

30. Ostashev, V., F. Gerdes, V. Mellert, and R. Wandelt. “Propagation of sound in a turbulent medium: II. – Spherical waves.” *The Journal of the Acoustical Society of America* 102: 2571-2578, 1997.

31. Ostashev, V., D. Wilson, L. Liu, D. Aldridge, N. Symons, and D. Marlin. “Equations for finite-difference, time-domain simulation of sound propagation in moving inhomogeneous media and numerical implementation.” *Journal of the Acoustical Society of America* 117(2): 503-517, 2005.

32. deRoo, F. and I. Noordhoek. “Harmonoisewp 2-reference sound propagation model.”*Fortschritte Der Akustik* 29: 354-355, 2003.

33. Delany, M. E. and E. N. Bazley. “Acoustical properties of fibrous absorbent materials.” *Applied Acoustics* 3: 105-116, 1970.

34. Chandler-Wilde, S. and D. Hothersall. “Efficient calculation of the Green’s function for acoustic propagation above a homogeneous impedance plane.” *Journal of Sound and Vibration* 180: 705-724, 1995.

35. Attenborough, K. “Sound propagation close to the ground,” *Annual Review of Fluid Mechanics* 34: 51-82, 2002.

36. Salomons, E. M. “Improved Green’s function parabolic equation method for atmospheric sound propagation.” *The Journal of the Acoustical Society of America* 104: 100-111, 1998.

37. Robertson, J. S., W. L. Seigmann, and M. J. Jacobson. “Low-frequency sound propagation modeling over a locally reacting boundary with the parabolic approximation.” *Journal of the Acoustic Society of America* 98: 1130-1137, 1995.

38. Stull, R. B. *An Introduction to Boundary Layer Meteorology*. Kluwer Academic Publishers, 1988.

39. Baik, J. J., J. J. Kim, and H. J. S. Fernando. “A CFD model for simulating urban flow and dispersion.” *Journal of Applied Meteorology* 42(11): 1636-1648, 2003.

40. Arizona Department of Transportation. *Progress Report no. 1, Arizona Department of Transportation (ADOT) Quiet Pavement Pilot Program (QPPP).* Arizona Dept. of Transportation, 23 December 2004.

BIBLIOGRAPHY

1. Harmonoise http://www.imagine-project.org/
2. Counihan, J., J. C. R. Hunt, and P. S. Jackson. "Wakes behind two-dimensional surface obstacles in turbulent boundary layers." *Journal of Fluid Mechanics* 64(3): 529-563, 1974.
3. Saurenman, H., J. Chambers, L. C. Sutherland, R. L. Bronsdon, and H. Forschner. *Atmospheric Effects Associated with Highway Noise Propagation*. Final Report 555. Arizona Dept. of Transportation, 2005.
4. Ovenden, N., S. Shaffer, and H. J. S. Fernando. "Impact of meteorological conditions on noise propagation from freeway corridors." *Journal of the Acoustical Society of America* 126: 25-35, July 2009.
5. Shaffer, S. *Investigations of Environmental Effects on Freeway Acoustics*. M.S. Thesis, Arizona State University, May 2009.